NASA TECHNICAL NOTE NASA TN D-2888

NASA TN D-2888

EXTRAGALACTIC RADIO SOURCES

by Wolfgang Priester and Johan Rosenberg

Goddard Space Flight Center
Greenbelt, Md.

NATIONAL AERONAUTICS AND SPACE ADMINISTRATION • WASHINGTON, D. C. • JULY 1965

NASA TN D-2888

EXTRAGALACTIC RADIO SOURCES

By Wolfgang Priester and Johan Rosenberg

Goddard Space Flight Center
Greenbelt, Md.

NATIONAL AERONAUTICS AND SPACE ADMINISTRATION

For sale by the Clearinghouse for Federal Scientific and Technical Information
Springfield, Virginia 22151 – Price $3.00

EXTRAGALACTIC RADIO SOURCES

by
Wolfgang Priester
Johan Rosenberg
Goddard Space Flight Center

SUMMARY

27812

This paper, based partly on lectures on radio astronomy given at the Columbia University Summer Institute in Space Physics in 1964, reports on the observations of radio galaxies and quasi-stellar radio sources (quasars). The basic physical processes responsible for continuous radio emission are studied.

Author

CONTENTS

EXTRAGALACTIC RADIO SOURCES*

by
Wolfgang Priester†
Johan Rosenberg
Goddard Space Flight Center

INTRODUCTION

The most challenging research problem in the field of radio astronomy at the present time is the attempt to understand the physical processes which cause certain extragalactic objects to emit radio radiation, the total power of which is up to six orders of magnitude larger than the radio emission of our own galactic system or of other "normal" galaxies. There are two kinds of those extremely strong extragalactic radio emitters known: the radio galaxies and the quasi-stellar radio sources. The latter name is nowadays abbreviated for convenience to "quasar" following a proposal by Chiu (Reference 1).

The radio sources called radio galaxies often show a double or multiple structure where the radio emission is observed to originate in large areas far outside of the optically observed galaxy. There are, however, also objects where a single area of radio emission is nicely centered around the optically observed galaxy. There are two basic problems in connection with the radio galaxies: first, to explain the observed brightness distribution, in particular in those cases where there are several or at least two centers of radio emission separated by distances which are much larger than the diameter of the optically observed parent-galaxy, and secondly, to find the physical process which is capable of providing the extremely large amount of total energy required for the production of the observed radio power.

The second problem is also the main problem for the quasi-stellar radio sources. Here the difficulties are even increased due to the comparatively small size of the areas of radio and light emission and due to the evidence that the total power emitted from these objects in the optical range is in the order of two orders of magnitude larger than the total light emission from the brightest giant galaxies. Further the radio emission of the quasars is equal to that of the brightest radio galaxies.

Let us say a few words on the terminology of radio sources. When John Hey in 1946, (Reference 2) discovered a point source in the constellation Cygnus, he called it a "radio star." In

*This report is partly based on lectures on radio astronomy given by W. Priester at the Columbia University Summer Institute in Space Physics, 1964.
†National Academy of Sciences–National Research Council Senior Research Associate with the Goddard Institute for Space Studies; on Leave from Bonn University.

the early 1950's about 100 radio sources were observed, but none of them identified with either a peculiar star or another optically known object. Then, in 1952, Walter Baade and Rudolph Minkowski identified the source in Cygnus and a few others with somewhat peculiar galaxies (Reference 3). Since the sources were distributed isotropically on the sky—if we disregard the few supernovae remnants in our own galaxy which are observable radio sources—it became apparent that the great majority or the radio sources were indeed galaxies with abnormally high radio emission and hence the term "radio star" was replaced by "radio galaxy." So far, more than 70 sources have been identified with galaxies, the radio emission of which is several orders of magnitude larger than the one from a normal galaxy like our own or M 31 (Andromeda nebula). The term "radio galaxy" is now generally used for these strong radio emitters.

The term "radio star," however, reappeared again at the 107th meeting of the American Astronomical Society in New York in 1960 when Allan Sandage announced that the radio source 3C 48 (No. 48 of the 3rd Cambridge catalog of radio sources) was identified with a 16th magnitude "star" in Triangulum by the perfect coincidence between optical and radio position. The identification was backed by the extremely small diameter of the radio source, less than 1". On a 90 minute exposure with the 200 inch telescope, the "star" is accompanied by a faintly luminous nebulosity measuring about 5" × 12", which, however, does by no means resemble a galaxy. The spectrum was considered to be very peculiar since no unequivocal identification with lines of known atoms or ions could be made immediately. By early 1963, five radio sources (3C 48, 147, 196, 273, and 286) were identified with similar star-like objects. All these radio sources have extremely small angular diameters of the order of one second of arc. The term "radio star" was, however, given up again, and replaced by quasi-stellar radio source when Maarten Schmidt (Reference 4) discovered that the observed optical emission line spectrum of the source 3C 273 is explainable if one accounts for a redshift of $\Delta\lambda/\lambda = 0.158$ corresponding to an apparent recession speed of 47,400 km/sec. This pointed strongly towards an extragalactic object at a great distance. There was therefore no good reason anymore to believe that the actual size of these objects was comparable to the size of a normal star.

In this paper we shall report essentially on the observational results on radio galaxies and quasars. Since there are no generally accepted views for the physical interpretation on the origin, evolution and energy supply of both kinds of objects, and since the proposed theories are likely to be subject to changes or improvement, we decided to leave out a detailed account of the proposed theoretical interpretations for the energy source of the objects. Instead we include a chapter treating the basic physical processes which are responsible for the generation of continuous radio emission. Both the radio galaxies and the quasars show typical non-thermal radio spectra which are generally believed to originate from magneto-bremsstrahlung of relativistic electrons spiraling in a magnetic field ("synchrotron emission"). For didactic purposes and comparison we treat also the origin of thermal spectra from Coulomb-bremsstrahlung in the chapter preceding the chapter on the synchrotron emission.

BASIC DEFINITIONS

Intensity and Flux

The *radiation intensity* $I_\nu\ (\theta, \phi)$ in a radiation field is defined as the amount of radiant energy, passing into the direction specified by (θ, ϕ) through a unit area A, perpendicular to this direction, during one time unit into a solid angle of one steradian within a frequency band of 1 c/s. Therefore in c.g.s. units the dimensions of intensity are:

$$\left[I_\nu\ (\theta, \phi)\right] = \text{erg cm}^{-2}\ \text{ster}^{-1}\ \text{sec}^{-1}\ (\text{c/s})^{-1}\ .$$

Although not explicitly mentioned, $I_\nu\ (\theta, \phi)$ also will depend in general upon time and the position of A. In Figure 1, then, the energy dE_ν, passing through the area $d\sigma$ into the solid angle $d\Omega$ during the time dt with frequencies between ν and $\nu + d\nu$, is

$$dE_\nu = I_\nu\ (\theta, \phi) \cos\theta\ d\sigma\ dt\ d\Omega\ d\nu\ . \tag{1}$$

The *radiation flux* S_ν is defined as the amount of energy passing through an area of 1 cm^2 in all directions during one time unit with a frequency bandwidth of 1 c/s. Hence the relation between flux and intensity is given by

$$S_\nu = \int_0 I_\nu\ (\theta, \phi) \cos\theta\ d\Omega \tag{2}$$

with the dimensions

$$\left[S_\nu\right] = \text{erg sec}^{-1}\ \text{cm}^{-2}\ (\text{c/s})^{-1}\ .$$

The symbol O denotes the whole sphere over which the integration has to be extended. If one expresses the element $d\Omega$ in spherical coordinates (θ, ϕ) (see Figure 1), we have $d\Omega = \sin d\theta\ d\phi$, and henceforth the flux is

$$S_\nu = \int_0^{2\pi} \int_0^{\pi} I_\nu\ (\theta, \phi) \sin\theta \cos\theta\ d\theta\ d\phi\ . \tag{3}$$

The average intensity F_ν of the radiation coming out of the unit area into one hemisphere denoted

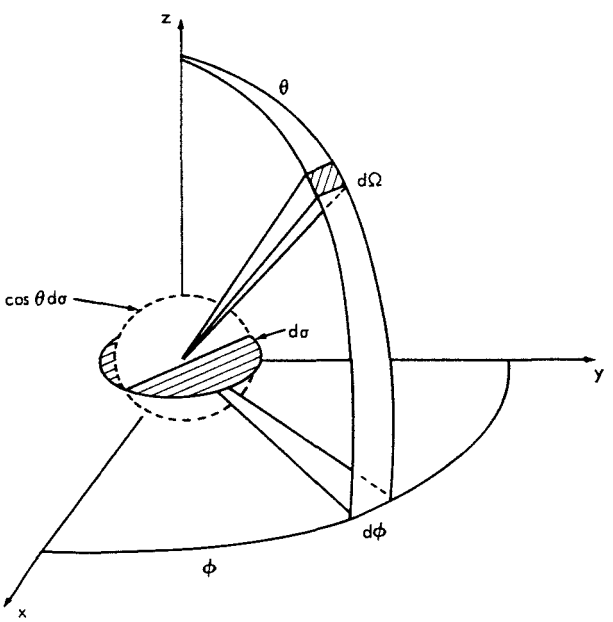

Figure 1—Test area $d\sigma$ in a spherical coordinate system (θ, ϕ). The dotted area is the projection of $d\sigma$ onto a plane perpendicular to the direction (θ, ϕ), where $d\Omega$ denotes an element of solid angle.

H is given by

$$F_\nu = \frac{\int_H I_\nu(\theta, \phi) \cos\theta \, d\Omega}{\int_H \cos\theta \, d\Omega} . \tag{4}$$

If the test area is situated in a field of *isotropic radiation*, i.e., if $I_\nu(\theta, \phi)$ is independent of (θ, ϕ), then $S_\nu = 0$. If there is no radiation coming in and the radiation going out is isotropic, we have

$$F_\nu = I_\nu(\theta, \phi) = \frac{S_\nu}{\pi} . \tag{5}$$

The *total flux* over all frequencies is given by

$$S = \int_0^\infty S_\nu \, d\nu . \tag{6}$$

Its c.g.s. units are $[S] = \text{erg cm}^{-2} \text{ sec}^{-1}$.

Brightness Temperature

We intend to find a relation between the emitted intensity at a certain frequency and the physical quantities determining the nature of the source. For this purpose it is convenient to compare the observed intensity with the intensity emitted by a black body at the same frequency. A black body is defined by the property that it absorbs all incident radiation at all frequencies. According to *Planck's Law* a black body having a temperature T radiates with an intensity given by

$$I_\nu \equiv B_\nu(\nu, T) = \frac{2h\nu^3}{c^2} \cdot \frac{1}{e^{h\nu/kT} - 1} \text{ erg sec}^{-1} \text{ cm}^{-2} \text{ ster}^{-1} (\text{c/s})^{-1} , \tag{7}$$

where

Planck's constant: $h = 6.6256 \pm 0.0005 \times 10^{-27}$ erg sec

Boltzmann's constant: $k = 1.38053 \pm 0.00006 \times 10^{-16}$ erg deg^{-1}

velocity of light: $c = 2.997925 \pm 0.000002 \times 10^{10}$ cm sec^{-1}.

The radiation of a black body does not depend on its material but only on the frequency and the temperature. The total radiant flux of a black body is given by Stefan-Boltzmann's Law

$$S = \int_0^\infty S_\nu \, d\nu = \sigma T^4 , \tag{8}$$

where the Stefan-Boltzmann's constant is $\sigma = 5.6697 \times 10^{-5}$ erg cm^{-2} sec^{-1} deg^{-4}.

In radio astronomy the temperatures of the sources will normally be over 100°K. The frequencies in use will in general be less than 3.10^4 Mc/s (corresponding to $\lambda \geq 1$ cm). Hence the quantity $h\nu/kT$ is generally <0.015. So we can safely approximate $e^{h\nu/kT}$ by the first two terms of the Taylor expansion:

$$e^{h\nu/kT} - 1 \approx \frac{h\nu}{kT} . \tag{9}$$

With this we obtain the *Rayleigh-Jeans approximation* of Planck's Law for $h\nu/kT \ll 1$:

$$B_\nu^{R.J.} = \frac{2h\nu^3}{c^2} \cdot \frac{kT}{h\nu} = \frac{2\nu^2 kT}{c^2} = \frac{2kT}{\lambda^2} \text{ erg cm}^{-2} \text{ sec}^{-1} \text{ ster}^{-1} (\text{c/s})^{-1} . \tag{10}$$

This approximation is very important in radio astronomy and will be used throughout these chapters. Note that the quantum theoretical factor has disappeared. This formula was actually already derived by Lord Rayleigh, using classical methods. Inserting appropriate values for k and c we find

$$B_\nu^{R.J.} = 3.07 \times 10^{-25} \nu^2 T \text{ erg sec}^{-1} \text{ ster}^{-1} (\text{c/s})^{-1} \text{ cm}^{-2} \tag{10a}$$

or

$$B_\nu^{R.J.} = 3.07 \times 10^{-28} \nu^2 T \text{ Watt m}^{-2} \text{ ster}^{-1} (\text{c/s})^{-1} \tag{10b}$$

in both cases taking $[\nu]$ = Mc/s and $[T]$ = °K.

A similar approximation exists for extremely high frequencies, i.e., for $h\nu/kT \gg 1$. Then $e^{h\nu/kT} - 1 \sim e^{h\nu/kT}$, and Planck's Law becomes

$$B_\nu^{W.} = \frac{2h\nu^3}{c^2} \cdot e^{-h\nu/kT} , \tag{11}$$

which is called *Wien's approximation.*

The *brightness temperature* $T_b(\nu)$ of a source for a certain frequency is defined as the temperature a black body must have to emit an equal intensity at that frequency, so

$$I_\nu \equiv B(\nu, T_b) \quad . \tag{12}$$

Here I_ν is the experimentally determined intensity. In radio astronomy, using the Rayleigh-Jeans approximation we find

$$T_b(\nu) = \frac{c^2}{2k} \cdot \frac{I_\nu}{\nu^2} \quad . \tag{13}$$

The brightness temperature corresponds only to the actual temperature if the source emits as a black body at that frequency, i.e., if the source is isothermal and if it absorbs all incident radiation. In all other cases the brightness temperature of a source will be a function of the frequency.

RADIATIVE TRANSFER

We will discuss here only a simplified case of radiative transfer applicable to most radio astronomical problems. A general treatment of the radiative transfer problem is given by S. Chandrasekhar (Reference 5). We will calculate the intensity of the radiation emitted by a layer of matter of finite thickness. The surface of the layer is assumed to be perpendicular to the line of sight.

The *absorption coefficient* κ_ν is defined as the fractional decrease of the intensity, when the radiation passes through a layer of 1 cm.:

$$\frac{dI_\nu}{I_\nu} = -\kappa_\nu \, ds \quad . \tag{14}$$

κ_ν is generally dependent upon the position of ds, and upon the frequency. It is $[\kappa_\nu] = cm^{-1}$. The emission coefficient ϵ_ν is defined as the amount of energy emitted by a unit volume per unit solid angle per second and per frequency band width of 1 c/s. Its dimensions are accordingly $[\epsilon_\nu]$ = erg sec^{-1} cm^{-3} $(c/s)^{-3}$ $ster^{-1}$.

With the notation as explained in Figure 2 we can write the equation of *radiative equilibrium*

$$I_\nu(s+ds)\, d\omega\, dt\, d\sigma\, d\nu - I_\nu(s)\, d\omega\, dt\, d\sigma\, d\nu = -\kappa_\nu \cdot I_\nu(s)\, ds\, d\omega\, dt\, d\sigma\, d\nu + \epsilon_\nu\, ds\, d\sigma\, dt\, d\omega\, d\nu$$

or

$$dI_\nu = -\kappa_\nu I_\nu\, ds + \epsilon_\nu\, ds \quad , \tag{15}$$

where I_ν, κ_ν and ϵ_ν depend upon ν and in general on the position of ds.

In our simplified consideration we assume that T is a function of s only. We further make the presumption that all the radiation arriving at s comes from regions close enough to s to have their temperatures approximated by T(s), that is, that changes of the temperature over the mean free path length of the radiation are small. This condition is called *local thermal equilibrium* (LTE). It is a very useful restriction, because then *Kirchhoff's Law* holds, saying that the ratio of the emission coefficient to the absorption coefficient is independent of the material and given by Planck's function:

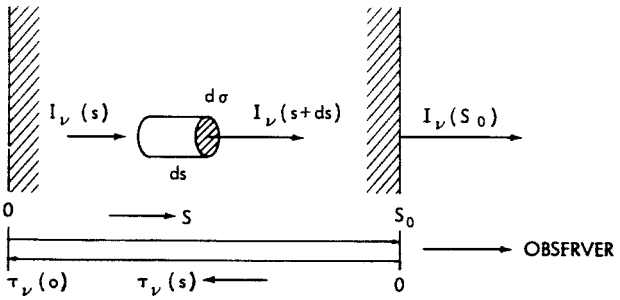

Figure 2—Simplified radiative transfer problem. The observer is assumed in the direction perpendicular to the surface of the layer, where s is the geometrical, and τ_ν the optical thickness.

$$\frac{\epsilon_\nu}{\kappa_\nu} = B_\nu \left[T(s)\right] . \tag{16}$$

This equation holds independent of the way in which the LTE is established, whether by radiation, convection or conduction. Note that $B_\nu \left[T(s)\right]$ is independent of the direction of the radiation. The *optical thickness* τ_ν is defined by

$$d\tau_\nu \equiv - \kappa_\nu \, ds . \tag{17}$$

Clearly we want τ_ν to be zero at $s = s_0$, assuming there is no absorption between the layer and the observer (see Figure 2). And for $s < s_0$, we want $\tau_\nu(s) > 0$. Hence

$$\tau_\nu(s) = \int_s^{s_0} \kappa_\nu \, ds . \tag{18}$$

Note that τ_ν is a dimensionless quantity. Division of Equation 15 by Equation 17 and using Equation 16 yields

$$\frac{dI_\nu(s)}{d\tau_\nu(s)} = I_\nu(s) - \frac{\epsilon_\nu(s)}{\kappa_\nu(s)} = I_\nu(s) - B_\nu \left[T(s)\right] . \tag{19}$$

Multiplying Equation 19 by $e^{-\tau_\nu(s)}$:

$$e^{-\tau_\nu(s)} \frac{dI_\nu(s)}{d\tau_\nu(s)} - e^{-\tau_\nu(s)} I_\nu(s) = - e^{-\tau_\nu(s)} B_\nu \left[T(s)\right] \tag{20}$$

and integrating between the limits $\tau_\nu = 0$ and $\tau_\nu = \tau_\nu(0)$ (i.e., $s = s_0$ and $s = 0$) we find

$$I_\nu(0) e^{-\tau_\nu(0)} - I_\nu(s_0) = - \int_0^{\tau_\nu(0)} B_\nu \, \tau_\nu(\tau_\nu) e^{-\tau_\nu} d\tau_\nu . \tag{21}$$

Assuming an *isothermal* layer we have $B_\nu [T(s)] = B_\nu (T)$ and hence $B_\nu (T)$ independent of $\tau_\nu (s)$. Inserting this in Equation 21 yields

$$I_\nu (0)\, e^{-\tau_\nu (0)} - I_\nu (s_0) = B_\nu (T) \left(e^{-\tau_\nu (0)} - 1 \right) . \tag{22}$$

Assuming that no radiation enters the layer from the rear side we then have the intensity of the radiation leaving the surface of an isothermal layer perpendicular to the surface:

$$I_\nu (s_0) = B_\nu (T) \left(1 - e^{-\tau_\nu (0)} \right) . \tag{23}$$

If $\tau_\nu (0) \gg 1$ so that $e^{-\tau_\nu (0)} \ll 1$, then the intensity for the emission from an optically thick layer $(\tau_\nu \gg 1)$ is

$$I_\nu = B_\nu = \frac{2\nu^2}{c^2} kT . \tag{24}$$

Hence the brightness temperature of the outgoing radiation is equal to the temperature of the layer

$$T_b = T . \tag{25}$$

If $\tau_\nu (0)$ is small $(\tau_\nu \ll 1)$ we approximate $e^{-\tau_\nu (0)}$ by $1 - \tau_\nu (0)$ and obtain the intensity of an emission from an optically thin layer

$$I_\nu = \tau_\nu (0) B_\nu = \tau_\nu (0) \frac{2\nu^2}{c^2} kT . \tag{26}$$

Accordingly the brightness temperature of the radiation is for $\tau_\nu (0) \ll 1$

$$T_b (\nu) = \tau_\nu (0)\, T . \tag{27}$$

From Equation 23 it also follows directly that in general

$$T_b (\nu) = T \left(1 - e^{-\tau_\nu (0)} \right) . \tag{28}$$

In an isothermal, homogeneous layer of ionized gas κ_ν is obviously independent of position and direction; thus we have

$$\tau_\nu (0) = \int_0^{s_0} \kappa_\nu \, ds = \kappa_\nu s_0 \tag{29}$$

and

$$I_\nu (s_0) = \frac{2\nu^2 kT}{c^2} \left(1 - e^{-\kappa_\nu s_0}\right) . \qquad (30)$$

From Equation 30 it is clear that the spectrum of a radio source will be determined by the dependence of the absorption coefficient κ_ν on the frequency ν.

There are two physical processes known which are generally believed to cause the radio emission with continuous spectra from celestial objects. One is a thermal process (Coulomb-bremsstrahlung), the other a non-thermal one (synchrotron emission or magneto-bremsstrahlung of relativistic electrons).

(1) The *Coulomb-bremsstrahlung,* i.e., the radiation emitted by electrons during Coulomb collisions, experienced when moving through the plasma with thermal (non-relativistic) velocities.

(2) The *Magneto-bremsstrahlung,* i.e., the radiation emitted by electrons which are accelerated in a magnetic field, while moving with non-relativistic (cyclotron emission) or relativistic velocities (synchrotron emission).

Thus we will derive two possible forms of spectra that radio sources may have. We can then compare observational data with these theoretical curves and decide whether the source is *thermal* (Coulomb-bremsstrahlung) or *non-thermal* (Magneto-bremsstrahlung), where we are still left with the possibility that the observed spectrum corresponds to neither of the two theoretical ones. All extragalactic radio sources (galaxies, radio galaxies and quasars) so far show spectra which can be interpreted as synchrotron emission spectra. We shall treat this process in a later chapter. First, for didactic reasons, we shall derive the thermal radio spectra from ionized gas-clouds.

THE ABSORPTION COEFFICIENT κ_ν FOR COULOMB-BREMSSTRAHLUNG

The Energy Emitted in a Free-Free Transition

In a completely ionized interstellar gas cloud without a magnetic field the radio frequency radiation with a continuous spectrum is merely due to free-free transitions of electrons in the Coulomb field of the ions. This radiation is called *thermal* radiation because the electrons involved have thermal velocities (i.e., energies of about 1 ev). As the radio frequencies will be emitted largely by electrons undergoing small accelerations, we will restrict ourselves to electrons having small deflections while passing a nucleus. This means the hyperbolae of the electron orbits are to be flat, which puts a lower limit on the collision parameter p (Figure 3). As the path on a flat hyperbola is nearly a straight line, we will disregard the y-component of the acceleration.

From classical electrodynamics (Reference 6), we know that the power passing through a unit area normal to the direction of the radiation is given by the Poynting vector at the position of

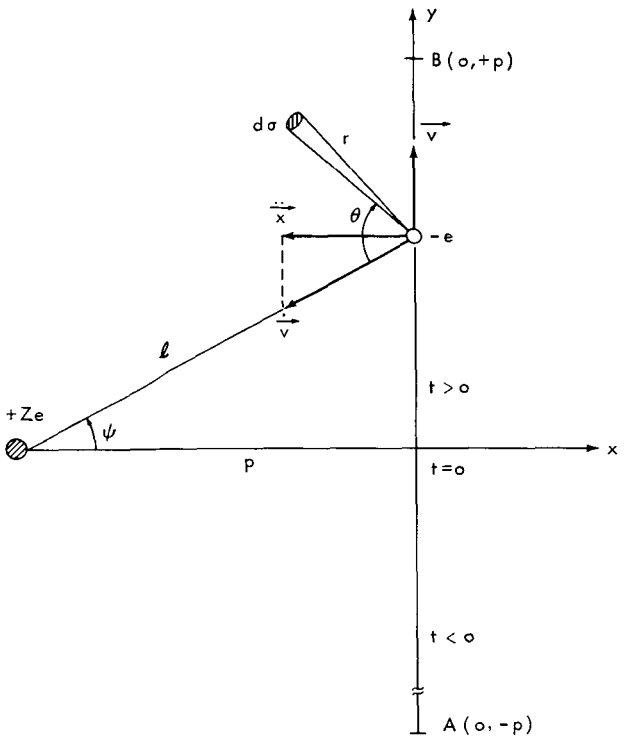

Figure 3—Free-free transition of an electron at a nucleus (Ze). The path of an electron passing a positively charged nucleus with a collision parameter p large enough to approximate the hyperbolic path by a straight line.

the area element. So

$$\frac{dQ}{d\sigma} = |\vec{S}| = \frac{c}{4\pi} [\vec{E} \times \vec{H}] . \qquad (31)$$

In the case of the accelerated electron, moving with non-relativistic speed, Equation 31 becomes

$$\frac{dQ}{d\sigma} = \frac{1}{4\pi} \frac{e^2 \sin^2\theta}{c^3} \frac{\ddot{x}^2}{r^2} \text{ erg cm}^{-2} \text{ sec}^{-1} \qquad (32)$$

if the y-component of the acceleration can be neglected. In Equation 32 the electron charge is $e = 4.80 \times 10^{-10}$ e.s.u.; θ denotes the angle between the direction of the emission and the acceleration, r is the distance between the electron and the area element under consideration. In Equation 32 we inserted $\ddot{x}$ for $\dot{v}$, according to our approximation.

The total energy emitted per unit time by the electron is

$$Q = \int_0 |\vec{S}| \, d\sigma = \int_0^{2\pi} \int_0^{\pi} \frac{1}{4\pi} \frac{e^2 \sin^2\theta}{c^3} \frac{\ddot{x}^2}{r^2} \cdot r^2 \sin\theta \, d\theta \, d\phi . \qquad (33)$$

The area element $d\sigma = r^2 \sin\theta \, d\theta \, d\phi$ in spherical coordinates. The axis ($\theta = 0$) of this system is given by the momentary direction of $\dot{\vec{v}}$. In our approximation this is always the direction of the negative x-axis. The integration yields

$$Q = \frac{2}{3} \frac{e^2}{c^3} \ddot{x}^2 \text{ erg sec}^{-1} . \qquad (34)$$

The Frequency Distribution

The frequency distribution of the emitted radiation can be obtained from a Fourier analysis. As illustrated in Figure 3 we define the time t with $t = 0$ at the moment of the closest approach between the electron and ion ($x = -p$, $y = 0$). Then $\ddot{x}(t)$ is symmetric in t, i.e., $\ddot{x}(+t) = \ddot{x}(-t)$, so we only need to use the cosine terms in the Fourier analysis of $\ddot{x}$. Here we follow closely the

analogous derivation by Kramers (Reference 7) (1923) for the x-ray spectrum. A detailed account can be found in the books of Unsöld (Reference 8) or Jackson (Reference 6). Formally the Fourier analysis can be expressed by

$$\ddot{x}(t) = \int_0^{\infty} C(\omega) \cos(\omega t)\, dt \ , \tag{35}$$

where

$$C(\omega) = \frac{1}{\pi} \int_{-\infty}^{+\infty} \ddot{x}(t) \cos(\omega t)\, dt \ . \tag{36}$$

Herein is $\omega = 2\pi\nu$; ν denotes the frequency. As Q contains the second power of $\ddot{x}$, we use Parseval's theorem to obtain the frequency spectrum of Q. We thus find

$$Q_\omega\, d\omega = Q_\nu\, d\nu = \frac{2e^2}{3c^3} \pi C^2(\omega)\, d\omega \ , \tag{37}$$

From general arguments in the Fourier analysis of a *pulse* of radiation, it is obvious that there will be hardly any contribution from frequencies with periods smaller than the duration of the pulse. Taking the characteristic transition time of the electron $t_1 = p/v$ [thus we assume $\ddot{x}$ to be negligible before the electron has reached A ($x = 0, y = -p$) or passed B ($x = 0, y = +p$) in Figure 3], we find for the contributing frequencies:

$$\omega < \frac{1}{t_1} = \frac{v}{p} \ . \tag{38}$$

As we have negligible emission for $|y| > p$, we have $-p/v < t < p/u$; so during the transition $|\omega t| < 1$ and we can approximate $\cos \omega t$ by 1. Since the acceleration according to Coulomb's Law is $\dot{v} = Ze^2/m\ell^2$, we have

$$\ddot{x} = \frac{Ze^2}{m\ell^2} \cos\psi(t) \qquad \text{(see Figure 3)} \ . \tag{39}$$

Inserting $1/\ell = \cos\psi(t)/p$ in $\ddot{x}$ we obtain

$$\ddot{x} = \frac{Ze^2}{mp^2} \cos^3\psi(t) \ . \tag{40}$$

From Equation 36 we find by using the fact that the contribution of $\ddot{x}(t)$ is only appreciable for $|t| < p/v$, i.e., where $\cos(\omega t) \approx 1$;

$$C(\omega) \approx \frac{1}{\pi} \int_{-\infty}^{+\infty} \ddot{x}(t)\, dt = \frac{1}{\pi} \int_{-\infty}^{+\infty} \frac{Ze^2}{mp^2} \cos^3\psi(t)\, dt \ . \tag{41}$$

We have $tg\psi(t) = v \cdot t/p$, and thus $dt = p/v \cos^2\psi \; d\psi$. Here we assume that v is approximately constant during $|t| < t_1$. Then Equation 41 becomes

$$C(\omega) = \frac{Ze^2}{\pi mp^2} \int_{-\pi/2}^{+\pi/2} \cos^3\psi \, \frac{p}{v\cos^2\psi} \, d\psi = \frac{Ze^2 \cdot 2}{\pi mpv} . \tag{42}$$

Using Equation 37 and remembering that $Q(\omega) \approx 0$ for $\omega > 1/t_1$ and that $C(\omega)$ corresponds to Equation 42 for $\omega < 1/t_1$ we find

$$Q_\nu \, d_\nu = \frac{2e^2}{3c^3} \pi \left(\frac{Ze^2 2}{\pi mpv}\right)^2 d\omega = \frac{16\, e^6 Z^2}{3c^3 m^2 p^2 v^2} \, d\nu \quad \text{for} \quad \nu < \frac{v}{2\pi p} \tag{43}$$

and

$$Q_\nu \, d\nu = 0 \quad \text{for} \quad \nu > \frac{v}{2\pi p} . \tag{44}$$

Note that in Equation 43, Q_ν is independent of ν. The Coulomb-bremsstrahlung spectrum of a single electron will therefore approximately look like a step function.

The Radio Spectrum of an Ionized Gas Cloud

To find the *spectrum of the radiation* emitted by the electrons in the interstellar gas, we have to sum over the appropriate collision parameters and over the Maxwellian distribution of the velocities, since these are the only variables appearing in the spectrum of one electron.

Let N_i be the number density of the ions, and N_e the number density of the electrons. Then the number (n_1) of Coulomb collisions, with collision parameters between p and $p + dp$, during one second, that an electron with velocity v will experience, is equal to the number of ions in a cylindrical ring of length v and of respective inner and outer radii, p and $p + dp$. So $n_1 = (v \cdot 2\pi p \cdot dp) \times N_i$ collisions sec^{-1} per electron. The number of collisions per cm^3 involving electrons with velocities between v and $v + dv$ and collision parameters between p and $p + dp$, $dN(v, p)$ is then

$$dN(v, p) = (v \cdot 2\pi p \cdot dp) \times N_i \times \left(N_e \, f(v) \, dv\right) \text{ collisions } cm^{-3} \; sec^{-1} , \tag{45}$$

where $f(v)$ denotes the Maxwell velocity distribution function. The energy emitted by a unit volume during one second in the frequency band between ν and $\nu + d\nu$ is then, using Equations 43

and 45 and the definition of the emission-coefficient

$$4\pi\,\epsilon_\nu = \int_{p_1}^{p_2}\int_0^\infty Q_\nu\,(p,\,v)\,dN(v,\,p)$$

$$= \int_{p_1}^{p_2}\int_0^\infty \frac{16e^6\,Z^2}{3c^3\,m^2\,p^2\,v^2}\,N_i\,N_e\,f(v)\,2\pi\,p\,v\,dp\,dv$$

$$= \frac{32\pi\,e^6\,Z^2\,N_i\,N_e}{3c^3\,m^2}\int_0^\infty \frac{f(v)}{v}\,dv\int_{p_1}^{p_2}\frac{1}{p}\,dp\ . \qquad (46)$$

From the kinetic theory of gases we know that the mean value of $1/v$ is $\overline{1/v} = \sqrt{2m/\pi kT}$; thus we have

$$\epsilon_\nu = \frac{8e^6\,Z^3\,N_i\,N_e}{3c^3\,m^2}\sqrt{\frac{2m}{\pi}}\cdot\frac{1}{\sqrt{kT}}\ln\frac{p_2}{p_1}\ \text{erg sec}^{-1}\ \text{cm}^{-3}\ (\text{c/s})^{-1}\ . \qquad (47)$$

We now have to insert appropriate values for p_2 and p_1. First we discuss the lower limit p_1.

We restricted ourselves in the entire discussion to flat hyperbolae, i.e., a small angle of deflection. We will take the upper limit of the deflection angle δ equal to $\pi/2$ radians. Then as $\text{tg}\ \delta/2 = Ze^2/p\cdot 1/mv^2$ we find

$$p_1 = \frac{Ze^2}{mv^2} = \frac{Ze^2}{3kT}\ . \qquad (48)$$

Another restriction on p_1 is the de Broglie wavelength of the electron. It has to be smaller than $2\pi p_1$, otherwise our classical derivation does not hold. Hence

$$p_1^* = \frac{h}{2\pi\,m\,u}\ . \qquad (49)$$

Comparing Equations 48 and 49 for some typical values in H II regions (ionized interstellar hydrogen clouds, which are the prototypes of thermal sources), we find, taking $T = 10^4\,°K$, $\bar{v} = 700$ km sec^{-1}, $Z = 1$

$$p_1 \simeq 6\times 10^{-8}\ \text{cm},\qquad p_1^* = 1.6\times 10^{-8}\ \text{cm}\ .$$

Generally we will find $p_1^* < p_1$, and we will therefore use p_1.

Now we discuss the upper limit p_2. In the discussion of the Fourier analysis of the spectrum of one electron we found that there will only be appreciable radiation with frequency ν for

$2\pi\nu < 1/t_1 = v/p$. This imposes an upper limit on p so

$$p_2 = \frac{\bar{v}}{2\pi\nu} \tag{50}$$

Furthermore, as we only want to consider two body collisions we want $p < r/2$ (where r is the average distance between the ions); r is given by $4\pi r^3 N_i/3 = 1$, so

$$p_2^* = \frac{1}{2}\left(\frac{4\pi}{3} N_i\right)^{-1/3} = \frac{1}{3.2 N_i^{1/3}} \tag{51}$$

Another restriction on p is given by the following. Around every ion we can picture a region in which its Coulomb field is undisturbed by the surrounding electrons and ions; outside this region however the other charges will "screen" its Coulomb field. An electron, passing this ion with a collision parameter p larger than the radius D of this "screening," clearly is not affected by the ion (Reference 9a and 9b). Taking the Debye length for the screening radius $D = \left(kT/4\pi e^2 N_e\right)^{1/2}$, we obtain a third upper limit

$$p_2^{**} = 6.9 \left(\frac{T}{N_e}\right)^{1/2} \text{ [cm]} \tag{52}$$

In the regions we are considering we have generally $p_2^{**} \gg p_2^*$. Example: in a H II region: $T = 10^4\,^\circ K$ and $N_i \approx N_3 < 10^3$ cm^{-3}. Hence $p_2^* \simeq 0.3$ cm, $p_2^{**} \simeq 20$ cm. Furthermore we find that for the H II regions, $p_2 < p_2^*$. In the corona of the sun, however, the density is much higher, so that there $p_2^* < p_2$; in that case we have to use p_2^* . We thus find for the emission coefficient, using Equations 47, 48, and 50,

$$\epsilon_\nu = \frac{8 e^6 Z^2}{3c^3 m^2} \sqrt{\frac{2m}{\pi k}} \cdot \frac{N_i N_e}{\sqrt{T}} \ln\left(\frac{(2kT)^{3/2} 3}{2\pi Ze^2 \sqrt{m}\,\nu}\right) \text{erg cm}^{-3} \text{ sec}^{-1} \text{ (c/s)}^{-1} \tag{53}$$

The derivation of Equation 53 holds only for two body collisions. Up to now no satisfactory treatment has been given of multiple scattering. We use Kirchhoff's Law (Equation 16) to derive the absorption coefficient κ_ν:

$$\kappa_\nu = \frac{4 e^6 Z^2}{3c\, m^2} \sqrt{\frac{2m}{\pi k}} \cdot N_i N_e \frac{1}{\nu^2 T^{3/2}} \ln\left(\frac{(2kT)^{3/2}}{4.22\pi Ze^2 \sqrt{m}\,\nu}\right) \tag{54}$$

The numerical values given in Equation 54 are taken from Elwert (Reference 10) and Oster (Reference 11). The logarithmic term in Equation 54 is not sensitive for variations in its constant. For example, if $T = 10^4\,^\circ K$, and $\nu = 2000$ Mc/s, a change in the constant by a factor 10 changes κ_ν only by 25%.

We are now in a position to determine the radio spectrum of an ionized cloud (H II region) by inserting κ_ν into Equations 24 and 25, and neglecting the slow variation with ν of the logarithmic term in κ_ν. In the case that the optical thickness $\tau_\nu = \kappa_\nu s_0 \ll 1$ we have the intensity I_ν independent of the frequency and proportional to $T^{-1/2}$:

$$I_\nu \sim \nu^0 \cdot T^{-1/2} \quad \text{for} \quad \tau_\nu \ll 1 . \tag{55}$$

For large optical thickness $\tau_\nu \gg 1$ we have

$$I_\nu \sim \nu^2 \cdot T \tag{56}$$

In this latter case the intensity corresponds to the intensity of a black body at the same temperature. As an example we calculate the surface intensity of the radio radiation emitted by an average H II region. The average corresponds to a list of 9 H II regions investigated by Sharpless and Osterbrook (Reference 12) and Oort (Reference 13): $T = 10^4$°K, $N_i = N_e = 10\ cm^{-3}$, $s_0 = 34$ pc. With these figures the optical thickness becomes $\tau_\nu = \kappa_\nu s_0 = 1.4 \times 10^{15}\ \nu^{-2}$ where the frequency ν is in (c/s). The optical thickness is equal to 1 for a frequency of $\nu = 37$ Mc/s. For smaller frequencies we have emission from an optically thick layer, therefore the intensity is proportional to ν^2; for larger frequencies than 37 Mc/s we have emission from an optically thin layer, where the intensity is nearly independent of the frequency. The shape of the spectrum is presented in Figure 4.

THE SYNCHROTRON EMISSION

The electromagnetic radiation from accelerated electrons with relativistic velocities was treated theoretically by Schott in 1912 (Reference 14). In the laboratory the radiation from electrons circling in a synchrotron was observed first in 1948. The importance of this process for the interpretation of the non-thermal radio radiation, observed from the galaxy and from the majority of the discrete radio sources, was realized by Alfvén and Herlofson (Reference 15) and by Kiepenheuer (Reference 16) in 1950. It is now generally believed that the non-thermal radio radiation is produced by Magneto-bremsstrahlung (synchrotron emission) from cosmic-ray electrons which spiral

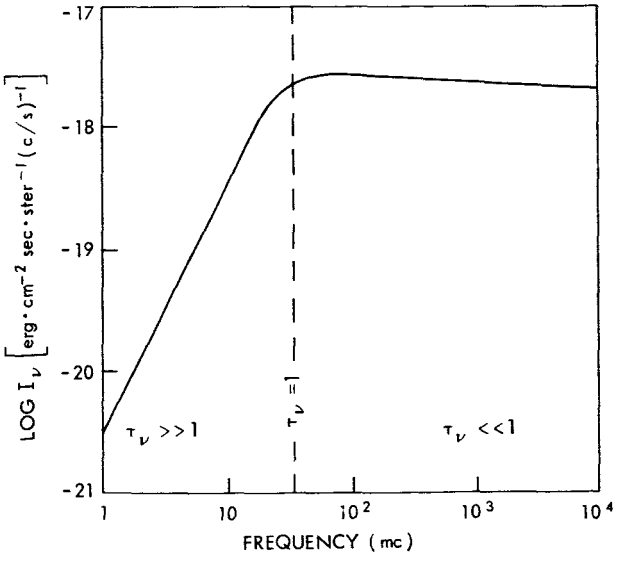

Figure 4—Thermal spectrum. The theoretical radio spectrum of a thermal source, with $T = 10^4$°K, $N_i = N_e = 10\ cm^{-3}$, $s_0 = 34$ pc.

in the magnetic fields in our galaxy. Ginzburg investigated in 1951 in an important paper (Reference 17) the relation between the observed spectral intensity distribution of the galactic radio emission and the energy spectrum of cosmic-ray electrons. At that time electrons were not yet observed in the cosmic rays. Ginzburg found that if the number of electrons is of the order of one percent of the number of cosmic-ray protons of the same energy then the observed radio spectrum could easily be explained by the synchrotron emission process. His prediction was nicely confirmed by the observations of Meyer and Vogt (Reference 18 and 19) and of Earl (Reference 20 and 21) who found a ratio of 3 ± 1 percent between the electrons and protons in the cosmic rays for energies above 500 Mev.

In the first section of this chapter we shall describe the radiation pattern of an accelerated electron in general. In the remaining part we then will derive the relation between the synchrotron spectrum of cosmic ray electrons and their energy distribution.

The Angular Distribution of the Radiation Emitted by an Accelerated Electron

In the non-relativistic case, i.e., $v/c \ll 1$, the power emitted by an electron accelerated in a magnetic field has the same momentary angular distribution as in the case of Coulomb-bremsstrahlung (refer to the previous section):

$$\frac{dP(\theta)}{d\Omega} = \frac{e^2 \dot{v}^2}{4\pi c^3} \sin^2\theta \text{ erg sec}^{-1} \text{ ster}^{-1} , \tag{57}$$

where θ is the angle between the direction of the acceleration and the considered direction of the radiation. $d\Omega$ is the element of the solid angle.

In the relativistic case $v/c \lesssim 1$, the angular distribution depends on $\dot{\vec{v}}$ and $\vec{v}$, and also on the general relativistic effect of the transformation from the rest frame of reference of the electron to the observer's frame. We will first discuss the dependence on $\dot{\vec{v}}$ and $\vec{v}$ and will then treat the relativistic effect on the observer.

From the didactic point of view it is preferable not to restrict the discussion on the acceleration of an electron in a magnetic field, but to treat two general cases of acceleration: (1) where the acceleration and the velocity have the same or opposite direction (linear accelerator): $\dot{\vec{v}} \parallel \vec{v}$, and (2) where the acceleration is perpendicular to the speed vector (synchrotron): $\dot{\vec{v}} \perp \vec{v}$.

We shall emphasize here the points which are important in our context, following essentially the treatment of the subject as given by Panofsky and Phillips (Reference 22) and Jackson (Reference 6). We shall use the following abbreviations throughout:

$$\beta = \frac{v}{c}$$

$$\gamma = \frac{E}{m_0 c^2}$$

hence

$$\gamma^2 = \frac{1}{1 - \beta^2} ,$$

where E is the total energy, m_0 the rest mass of the electron, c the speed of light.

We treat first the case: $\dot{\vec{v}} \parallel \vec{v}$:

The power radiated per unit solid angle has the following pattern (Reference 6):

$$\frac{dP}{d\Omega} = \frac{e^2 \dot{v}^2}{4\pi c^3} \frac{\sin^2 \theta}{(1 - \beta \cos \theta)^5} \text{ erg sec}^{-1} \text{ster}^{-1} . \quad (58)$$

Note that now θ is defined as the angle between the velocity and the considered direction of the radiation. The direction of $\vec{v}$ and $\dot{\vec{v}}$ which here are either parallel or anti-parallel is clearly an axis of symmetry. In the non-relativistic case we had a toroidal radiation pattern with a $\sin^2 \theta$ cross section. Now in the relativistic case the toroidal pattern is distorted and bent over into the direction of the speed vector, while maintaining that the emission is zero in the axis of symmetry. Illustrations are given in Figures 5 and 6. From Equation 57 the angle of peak intensity is easily found:

$$\cos \theta_{max} = \frac{1}{3\beta} \left(\sqrt{1 + 15\beta^2} - 1 \right) \quad (59)$$

For $\beta \to 1$ we have

$$\theta_{max} = \frac{1}{2\gamma} . \quad (59a)$$

The power in the direction θ_{max} increases very rapidly with increasing γ. It is proportional to γ^8. The total power, obtained by integrating (2) over all solid angles is

$$P = \frac{4}{3} \frac{e^2 \dot{v}^2}{c^3} \gamma^6 . \quad (60)$$

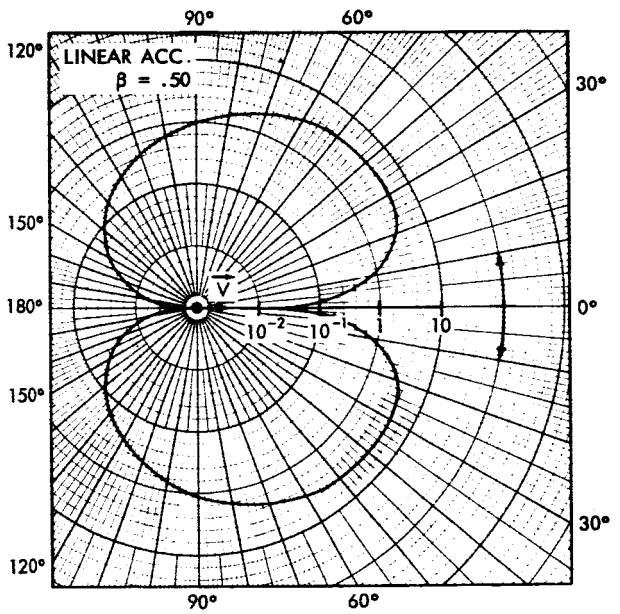

Figure 5—Radiation of a linearly accelerated electron. The angular distribution of the electromagnetic radiative power emitted by a linearly accelerated electron with $\beta = v/c = .50$. The logarithmic scale has arbitrary units.

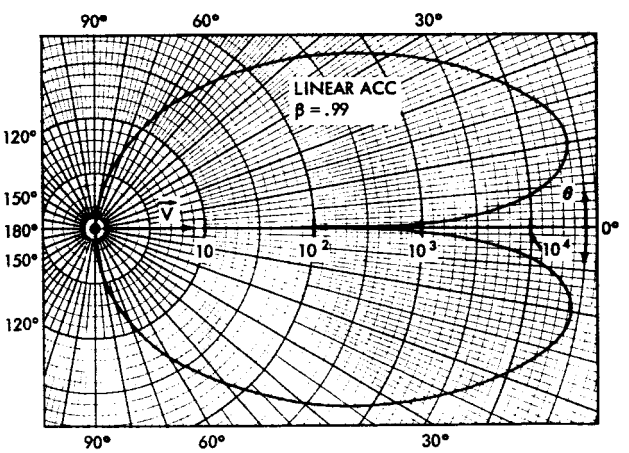

Figure 6—Radiation of a linearly accelerated electron (the same as Figure 5 with $\beta = v/c = .99$). The logarithmic scale has arbitrary units, different from those of Figure 5.

More important for the application in radio astronomy is the second case: $\dot{\vec{v}} \perp \vec{v}$. This is the case when an electron moves in a magnetic field where the field vector is perpendicular to the speed vector. We define a coordinate system in the following way: the z-axis in the direction of the velocity vector, the x-axis in the direction of acceleration. The corresponding polar coordinate system (r, φ) is determined by θ measured from the positive z-axis, ϕ in the xy-plane with $\phi = 0$ in the positive x-axis. Then the power per steradian in the frame of the electron is given by

$$\frac{dP}{d\Omega} = \frac{e^2 \dot{v}^2}{4\pi c^3} \cdot \frac{1}{(1 - \beta \cos\theta)^3} \left[1 - \frac{\sin^2\theta \cos^2\phi}{\gamma^2 (1 - \beta \cos\theta)^2}\right], \tag{61}$$

where again $\beta = v/c$, $\gamma = E/m_0 c^2$.

For $\gamma \gg 1$, $\beta \sim 1$, we can approximate (5) by

$$\frac{dP}{d\Omega} = \frac{2}{\pi} \cdot \frac{e^2 \dot{v}^2}{c^3} \gamma^6 \frac{1}{\left(1 + \gamma^2\theta^2\right)^3} \left[1 - \frac{4\gamma^2\theta^2 \cos^2\phi}{\left(1 + \gamma^2\theta^2\right)^2}\right]. \tag{62}$$

In this case, we do not have an axis of symmetry. Here we find the maximum power at $\theta = 0$, the direction of the speed vector. We have two directions where *no* emissions takes place: in the xz-plane ($\phi = 0$) if $\cos\theta = \beta$, i.e., $\theta \approx 1/\gamma$.

In Figures 7 and 8 the angular distribution of the radiation for $\beta = 0.99$ and $\gamma = 1.4$ is given in the xz-plane ($\phi = 0$) and the yz-plane ($\phi = 90°$). It is interesting to compare this with the non-relativistic case and to note the way the toroidal pattern with $\dot{\vec{v}}$ as axis is deformed by bending it over in the direction of $\vec{v}$. This results in side lobes in the xz-plane. In the xz-plane the main beam is confined within an angle of $2/\gamma$. It is therefore reasonable to define the characteristic

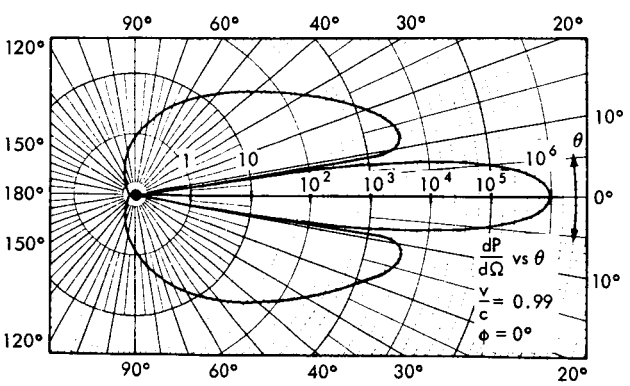

Figure 7—Synchrotron radiation. The angular distribution of the electromagnetic radiative power emitted by a circularly accelerated electron with $\beta = .99$ in the plane $\phi = 0$, i.e., the plane defined by $\dot{\vec{v}}$ and $\vec{v}$. The power is given by the radius vector in an arbitrary logarithmic scale.

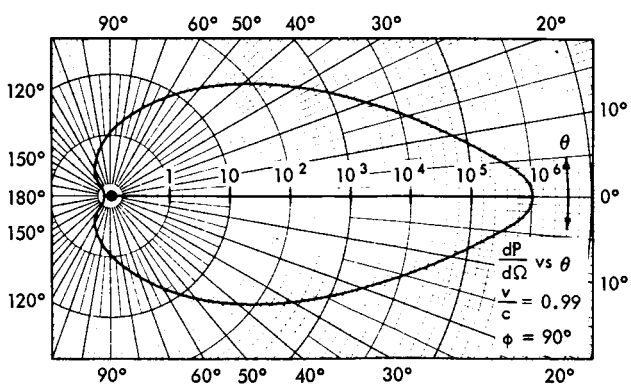

Figure 8—Synchrotron radiation (the same as Figure 7 but now with $\phi = 90°$). The plane is perpendicular to the one defined by $\dot{\vec{v}}$ and $\vec{v}$. The scale is the same as in Figure 7.

width of the main beam by

$$\theta_0 = \frac{m_0 c^2}{E} = \frac{1}{\gamma} . \tag{63}$$

For $\gamma \gg 1$, the power at $\theta = 0$ varies as γ^6. The total power over all solid angles is again obtained by integrating Equation 61. We then find

$$P = \frac{2}{3} \frac{e^2 \dot{v}^2}{c^3} \left(\frac{E}{m_0 c^2} \right)^4 = \frac{2}{3} \frac{e^2 \dot{v}^2}{c^3} \gamma^4 \text{ erg sec}^{-1} . \tag{64}$$

Note that the total radiation power of a linearly accelerated electron varies with γ^6, whereas the power emitted by an electron in a circular orbit varies with γ^4. However if we write Equations 60 and 64 in terms of the change in momentum, i.e., the applied force, and use the *relativistic* expression for force, we find $P = \left(2e^2/3m_0^2 c\right)(d\vec{p}/dt)^2$ for a linearly accelerated electron and $P = \left(2e^3 \gamma^2/3m_0^2 c\right)(d\vec{p}/dt)^2$ for an electron in a circular orbit. Table 1 gives some values of β with the corresponding values of γ and the characteristic beam width.

Table 1

Properties of Electrons and Protons Moving in a Magnetic Field.

Particle Types	Velocity (km/sec)	β	γ	$\theta_{1/2}$	T	E (ev)	R_L (km) (for H = 10^{-5} Gauss)
Thermal Electrons	10^2	$\frac{1}{3000}$	~1	—	200°K	5×10^5	0.57
	10^3	$\frac{1}{300}$	~1	—	2×10^4°K	5×10^5	5.7
Relativistic Electrons	1.5×10^5	.5	1.14	50°	—	6×10^5	10^3
	2.7×10^5	.9	2.3	25°	—	1.18×10^6	3.4×10^3
	~c	.99	7.1	8°	—	3.6×10^6	11.9×10^3
	~c	~1	2000	5×10^{-4} rad	—	10^9	3.4×10^6 = ~10^{-7} pc
	~c	~1	2×10^{12}	5×10^{-13} rad	—	10^{18}	3×10^{15} = ~100 pc
Thermal Protons	23	7.5×10^{-5}	~1	—	2×10^4°K	9.4×10^8	250
Relativistic Protons	1.5×10^5	.5	1.14	50°	—	1.09×10^9	1.8×10^6
	~c	.99	7.2	8°	—	6.6×10^9	22×10^6
	~c	~1	10^9	10^{-9} rad	—	10^{18}	100 pc

The Larmor Circle

If an electron enters a homogeneous magnetic field, the orbit will be a spiral in the non-relativistic case, the radius of the circle determining the spiral given by

$$R_L = \frac{m_0 v c}{eH_\perp} \text{ cm} . \tag{65}$$

$H_\perp$ is the component of $\vec{H}$ normal to $\vec{v}$. In the relativistic case m_0 would be replaced by $m = m_0 \gamma$ (see Equation 69).

The angular frequency called *Larmor* frequency is given by

$$\omega_{H,0} = \frac{eH_\perp}{m_0 c} \text{ rad sec}^{-1} \tag{66}$$

In the non-relativistic case the electron radiates like a dipole, with a frequency determined by the Larmor frequency; this emission is called *cyclotron emission* or *gyromagnetic emission.* Its frequency is (in Mc):

$$\nu_{H,0} \simeq 2.8 \times H_\perp \text{ Mc} , \tag{67}$$

where $H_\perp$ is in gauss. Cyclotron radiation is circularly or elliptically polarized in the direction normal to $H_\perp$. To obtain radiation with radio frequencies, i.e., 10 - 10^4 Mc, we would thus need magnetic fields of 1 - 10^4 gauss, which are highly improbable field strengths in interstellar space. In the sun's atmosphere, these field strengths are possible but a more detailed treatment has shown that only the harmonics of $\nu_{H,0}$ can be observed, not the fundamental frequency.

In the *relativistic case* we have

$$\omega_{H,\beta} = \frac{eH_\perp \sqrt{1 - \frac{v^2}{c^2}}}{c m_0} = \frac{eH_\perp}{m_0 c} \cdot \frac{m_0 c^2}{E} = \frac{eH_\perp}{m_0 c} \cdot \frac{1}{\gamma} \text{ rad sec}^{-1} \tag{68}$$

So $\omega_{H,\beta} < \omega_{H,0}$. We thus find that the angular frequency decreases compared to the non-relativistic case, even though the velocity is increasing; hence the radius increases. As $2\pi R_L = v/\nu$, we have the Larmor radius

$$R_L = \frac{v}{\omega} = \frac{m_0 cv}{eH_\perp} \gamma \text{ cm} . \tag{69}$$

Note that in Equation 69, for $\gamma \gg 1$, $v \approx c$; hence

$$R_L = \frac{m_0 cv}{eH_\perp} \cdot \frac{E}{m_0 c^3} \sim \frac{E}{eH_\perp} ; \tag{70}$$

so in that case R is independent of the mass of the particle.

Table 1 gives a few values for the Larmor radii of different particles for different energies. The field-strength used is 10^{-5} gauss. This value is obtained by assuming that there exists equilibrium between the energy density of the magnetic field and of the turbulent motions of the clouds in the galaxies.

The Duration of the Observed Pulse of Radiation

Equation 61 states that for $\gamma \gg 1$, the radiation is emitted mainly into a narrow cone pointing into the direction of the instantaneous speed of the electron. From Equation 63 we know that the characteristic angular width of the cone is equal to

$$\theta_0 = \frac{1}{\gamma} . \tag{71}$$

In order to sweep across a distant observer the cone has to move from A to B in Figure 9. In the reference frame of the electron this will take time $\Delta t = R\theta_0/c$, where we assume $\beta \approx 1$. In other words the duration of the pulse observed by the observer will last in the *reference frame of the electron* (using Equations 70 and 71),

$$\Delta t = \frac{R\theta_0}{c} = \frac{m_0 c}{eH_\perp} . \tag{72}$$

A signal emitted at time t at $\vec{R}(t)$ is received at time t' by the observer at $\vec{r}$ (Figure 9)

$$t' = t + \frac{|\vec{r} - \vec{R}(t)|}{c} \tag{73}$$

and as $|\vec{r} - \vec{R}(t)| = \sqrt{[\vec{r} - \vec{R}(t)]^2}$,

$$\frac{dt'}{dt} = 1 - \frac{1}{c} \frac{[\vec{r} - \vec{R}(t)]}{|\vec{r} - \vec{R}(t)|} \cdot \frac{d\vec{R}(t)}{dt} \tag{74}$$

Here $[\vec{r} - \vec{R}(t)]/|\vec{r} - \vec{R}(t)|$ is the unit vector into the direction of the observer, and $d\vec{R}(t)/dt = \vec{v}(t)$. Hence $dt'/dt = 1 - (v/c)\cos\theta$. As Δt is

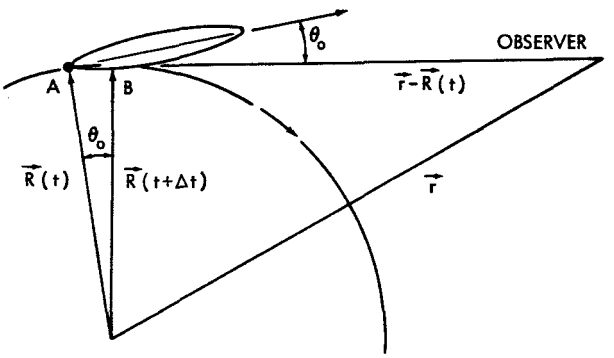

Figure 9—Pulse time. The relation between the characteristic beam width and the characteristic time during which it is observed at a distance $\vec{r}$.

very small we can approximate $\Delta t'$ by

$$\Delta t' = \left(1 - \frac{v}{c} \cos \theta_0\right) \Delta t \tag{75}$$

with $\theta_0 = 1/\gamma = \sqrt{1 - v^2/c^2}$. For $\theta_0 \ll 1$, $\cos \theta_0 = \sqrt{1 - \theta_0^2} = v/c = \beta$, so the characteristic time for the duration of the pulse for the *observer* is

$$\Delta t' = \left(1 - \frac{v^2}{c^2}\right) \cdot \Delta t = \left(\frac{m_0 c^2}{E}\right)^2 \cdot \frac{m_0 c}{eH_\perp} . \tag{76}$$

The Spectral Distribution

According to general properties of Fourier integrals, the spectrum will have appreciable intensity up to a *critical frequency* given approximately by the inverse of the *characteristic time*. We will define the critical angular frequency ω_c as

$$\omega_c \equiv \frac{1}{\frac{2}{3} \Delta t'} = \frac{3}{2} \frac{eH_\perp}{m_0 c} \left(\frac{E}{m_0 c^2}\right)^2 \text{ rad sec}^{-1} \tag{77}$$

or

$$\omega_c = \frac{3}{2} \omega_{H,0} \gamma^2 = \frac{3}{2} \omega_{H,\beta} \gamma^3 . \tag{78}$$

Since the spectrum in fact does not decrease abruptly to zero at a certain frequency, we shall find slightly different definitions for the critical frequency in the literature. Here we used Schwinger's definition, which is most commonly used in radioastronomy [see, for example, Oort (Reference 13) and Jäger and Wallis (Reference 23)]. Ginzburg, however, used as critical angular frequency a value which is only 2/3 of the one given in Equation 77. Jackson's value is twice as large as ω_c in Equation 77.

By Equation 67 we have for the critical frequency $\nu_c = 4.2\ H_\perp \cdot \gamma^2$ Mc, where H is in gauss. In order to obtain radiation in the radio frequency range (10 - 10^4 Mc) from relativistic electrons γ has to be between 500 and 15,000 if we assume a magnetic field of 10^{-5} gauss. This range for γ corresponds to energies from 2.5×10^8 to 8×10^{10} ev. It is interesting to note what energies would be required for relativistic protons if one wants to obtain synchrotron radiation in the same radio frequency range from them. From Equation 77 one can easily see that the proton energies must be larger by $(m_p/m_0)^{3/2}$, where m_p is the rest mass of the proton. Therefore the energy range required for protons would be from 2×10^{13} to 6×10^{15} ev.

The frequency distribution of the total energy of the pulse as observed by the observer is obtained by Fourier analysis of the emitted power. We omit here the details and refer the reader interested in them to the paper by Schwinger (Reference 24).

The frequency distribution is given by

$$P_\nu = \frac{\sqrt{3}\, e^3}{m_0 c^2} H_\perp F\left(\frac{\nu}{\nu_c}\right) \text{ erg sec}^{-1} (c/s)^{-1} , \tag{79}$$

where $\nu_c = \frac{\omega_c}{2\pi} = \frac{3}{4\pi} \frac{eH_\perp}{m_0 c} \gamma^2$, and

$$F\left(\frac{\nu}{\nu_c}\right) = \int_{\nu/\nu_c}^{\infty} K_{5/3}(x)\, dx . \tag{80}$$

$K_{5/3}$ is a special case of the Airy integral (or modified Bessel function or modified Hankel function). Oort (Reference 13) gives a graph of the frequency distribution.

G. Wallis (Reference 25) found a very convenient approximation of the Airy integral. It is sufficiently accurate for all applications in radioastronomy:

$$F_W = 1.78 \cdot \left(\frac{\nu}{\nu_c}\right)^{0.3} \cdot e^{-\nu/\nu_c} . \tag{81}$$

F and F_W have the same maximum values at the same value of ν/ν_c; furthermore $\int_0^\infty F_W\, d\nu = 0.993 \int_0^\infty F\, d\nu$. Actually the spectrum of one electron is not continuous, but a discrete spectrum with values of P_ν different from 0 only in the harmonics of the Larmor frequency. However as $\gamma > 500$ and $\omega_c = 3/2\ \omega_{H,0}\ \gamma^2$ the harmonics of $\omega_{H,0}$ are so closely spaced in the region of ω_c that we can regard P_ν as a continuous spectrum (Reference 24).

The Spectrum of the Radio Frequency Radiation Emitted by the Galactic Cosmic Ray Electrons

In analogy to the observed energy distribution of cosmic ray protons we assume a differential energy distribution for the relativistic electrons as given by

$$N_e(E)\, dE = A \cdot E^{-g}\, dE\, cm^{-3} , \qquad [N_e] = cm^{-3}\ erg^{-1} , \tag{82}$$

where N_e is the number density of cosmic ray electrons with energies between E and E + dE, and g is called the spectral index of the energy spectrum, A is a constant determining the absolute numbers. If we now assume that along the line of sight, the magnetic fields in general are distributed at random, then we can regard the synchrotron radiation as being isotropic, if we take an average over a large range. $P_\nu(E)$ is the total energy emitted per sec by an electron, so we can say that $4\pi I_\nu(E) = P_\nu(E)$, where $I_\nu(E)$ denotes the average intensity of the radiation of an electron in any direction, i.e., $I_\nu(E)$ is the isotropic intensity. We now want to calculate the intensity of the synchrotron radiation emitted along the line of sight as received by an observer. Note that the intensity of radiation is not dependent upon the distance between the observer and the source, as

long as we assume that there is no absorption along the line of sight. Jäger and Wallis (Reference 23) confirmed that absorption is negligible for the wavelengths and densities we are concerned with. Combining the spectrum P_ν emitted from a relativistic electron having the energy E with the energy distribution of the electrons N_e, we obtain the intensity of the radiation by integrating over the line of sight and over the cosmic ray energy range:

$$I_\nu = \int_0^\infty \int_{E_0}^\infty \frac{P_\nu(E)}{4\pi} N_e(E, r)\, dE\, dr \text{ erg cm}^{-2} \text{ sec}^{-1} \text{ ster}^{-1} (\text{c/s})^{-1} . \quad (83)$$

In order to estimate the synchrotron radiation from our galaxy for a certain direction we assume for simplicity that $N_e(E)$ is independent of r, for $0 < r < r_0$, where r_0 denotes the border of the galaxy along the line of sight, and $N_e(E) = 0$ for $r > r_0$. Then Equation 83 becomes

$$I_\nu = \frac{r_0}{4\pi} \int_{E_0}^\infty P_\nu(E) N_e(E)\, dE . \quad (84)$$

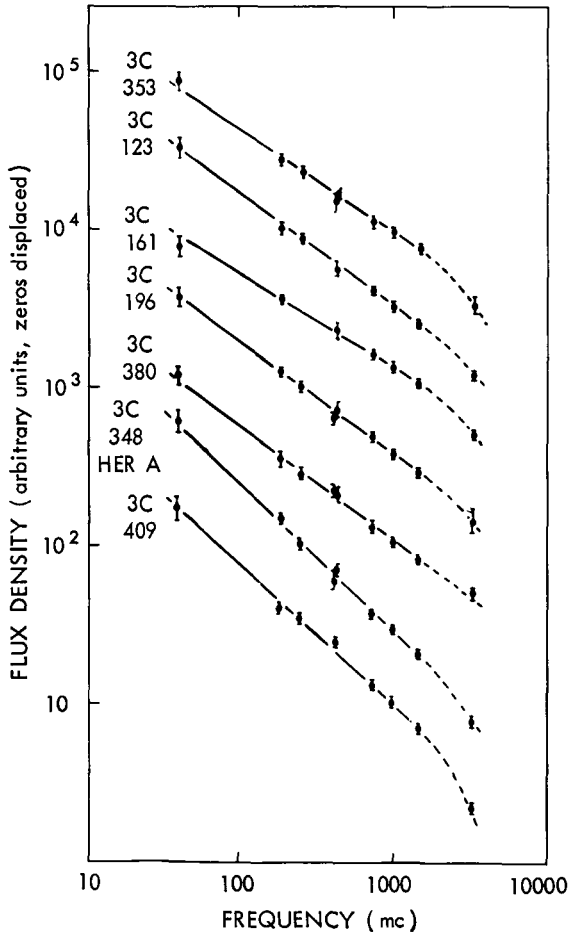

Figure 10—Non-thermal spectra. A few examples of radio spectra of non-thermal radio sources (Reference 26a).

If we observe a radio source which emits synchrotron radiation and appears under the solid angle Ω, then the received flux S_ν is

$$S_\nu = I_\nu \Omega$$

$$= \Omega \int_{\text{vol}} \int_{E_0}^\infty \frac{P_\nu(E)}{4\pi} N_e\left[E(x, y, z)\right] dE\, dx\, dy\, dz \quad (85)$$

Here we assumed already a random distribution of the magnetic fields in the source, and the absence of absorption throughout the source, i.e., that the mean free path of the photons is much larger than the diameter of the source. Assuming again that $N_e(E)$ is independent of (x, y, z) we find

$$S_\nu = \frac{\Omega\, \text{vol}}{4\pi} \int_{E_0}^\infty P_\nu(E) N_e(E)\, dE , \quad (86)$$

where vol designates the volume of the source.

Returning to the intensity of the galactic synchrotron radiation Equation 84 we obtain by

using Equations 79 and 82 for the spectrum P_ν and the differential energy distribution N_e, respectively:

$$I_\nu = \frac{r_0}{4\pi} \frac{\sqrt{3}\, e^3}{m_0 c^2} AH \int_{E_0}^{\infty} F\left(\frac{\nu}{\nu_c (E)}\right) E^{-g}\, dE \tag{87}$$

We now use the Wallis approximation for $F(\nu/\nu_c)$, and abbreviate $\sqrt{3}\, e^3/m_0 c^2$ with C. We furthermore abbreviate the expression for the critical frequency $\nu_c = \epsilon E^2$ where ϵ stands for $(3/4\pi)(eH/m_0^3 c^5)$. Then Equation 87 becomes

$$I_\nu = \frac{1.78}{4\pi} r_0 C A H \nu^{0.3} \epsilon^{-0.3} \int_{E_0}^{\infty} E^{-(g+0.6)}\, e^{\nu/-\epsilon E^2}\, dE \,. \tag{88}$$

If we substitute $E = \sqrt{\nu/\epsilon}\, x$ we obtain

$$I_\nu = \frac{1.78}{4\pi} r_0 C A H \left(\frac{\nu}{\epsilon}\right)^{-(g-1)/2} \int_{x_0}^{\infty} x^{-(g+0.6)}\, e^{-1/x^2}\, dx \,. \tag{89}$$

This reveals that the intensity of the synchrotron radiation should be proportional to $\nu^{-(g-1)/2}$ provided that our assumptions are valid. In fact, the observed spectra of the non-thermal component of the galactic radio radiation and the non-thermal extragalactic sources can be reasonably well represented by a simple power law:

$$I_\nu \text{ (observed)} = \nu^{-\alpha} \,. \tag{90}$$

In order to prove that the non-thermal radio radiation stems from the synchrotron process, we have to show that if we equate the observed spectral index α to the theoretical value $(g-1)/2$, and also the observed intensity at one selected frequency to the theoretical intensity, we obtain reasonable values for both the spectral index of the energy spectrum (i.e., "g") and the number densities of the cosmic ray electrons.

Figure 10 shows 7 typical spectra of non-thermal radio sources (Reference 26b). The spectral indices are (from top to bottom): α = 0.63, 0.69, 0.59, 0.71, 0.70, 0.90 and 0.88. The average spectral index taken over a larger sample of typical sources is 0.7. The spectrum of the galactic radio radiation is slightly less steep. From the survey by Baldwin (Reference 27) at 81 Mc/s, Dröge and Priester (Reference 28) at 200 Mc/s and McGee, Stanley and Slee (Reference 29) at 400 Mc/s, one finds α = 0.61. The same value was obtained by Westerhout (Reference 30a) from a comparison of a larger number of sky surveys.* If we take α = 0.7 we have to require that the index g of the energy distribution of cosmic ray electrons in the non-thermal radio sources is

*In 1962 Turtle et al. (Reference 30b) again investigated the spectra of the radiation from the galactic halo and the galactic disc. They obtained a slight change of the spectral index α with the wavelength: a smaller value at the longer wavelengths. For simplicity we shall only discuss a constant value for the spectral index.

$g = 2.4$. This value is in reasonably good agreement with the observed energy spectrum of cosmic ray protons in the energy range from 10^9 to 10^{10} ev. In the literature the integrated energy spectrum N_e^* of the cosmic ray particles for energies larger than a certain limit E_0 is usually given. It is

$$N_e^* (E > E_0) = \int_{E_0}^{\infty} N_e (E)\, dE = \frac{A}{G} E_0^{-G} \tag{91}$$

where $G = g - 1$.

Cosmic ray electrons were discovered in 1960 by Meyer and Vogt (References 18 and 19) with an electronic detector and by Earl with a cloud chamber in a sky-hook balloon at an altitude of about 36 km (Reference 21). The lower energy limit was $E_0 = 5 \times 10^8$ ev. The observed flux was $f = 32 \pm 10$ el/m^2 ster sec. If we assume isotropy, we are able to calculate N_e^* from

$$N_e^* = \frac{4\pi}{c} f = 1.3 \times 10^{-12} \text{ cm}^{-3} \tag{92}$$

for $E > E_0 = 5 \times 10^8$ ev.

We now assume that the same power law, as observed for the energy distribution of cosmic ray protons, also applies for the electrons. Hence for 10^9 ev $< E < 10^{10}$ ev, we take $g = 2.4$. Using Equation 91 we find:

$$N_e^* (E > 5 \times 10^8 \text{ ev}) = \frac{A}{1.4} E_0^{-1.4} = 1.3 \times 10^{-12} \text{ cm}^{-3} \tag{93}$$

or

$$A = 8.2 \times 10^{-17} \text{ erg}^{1.4} \text{ cm}^{-3} .$$

We are now in a position to calculate the intensity of the galactic synchrotron radiation for a selected direction and frequency and to compare the result with the observed intensity. For the value $g = 2.4$ the integral in Equation 89 is immediately calculated if we integrate from 0 to ∞. One can easily see that the error introduced by integrating from 0 can be neglected.

$$\int_0^{\infty} x^{-3} e^{-1/x^2} dx = \frac{1}{2} \int_0^{\infty} e^{-u} du = \frac{1}{2} . \tag{94}$$

Inserting the constants into Equation 89 and remembering that ϵ involved H, we find

$$I_\nu = 2.0 \times 10^{-26} H^{1.7} r_0 \nu^{-0.7} . \tag{95}$$

If we now take $H = 10^{-5}$ gauss and $r_0 = 2 \times 10^4$ parsec $= 6 \times 10^{22}$ cm, corresponding to a galactic longitude $\ell^{II} = 30°$ we have

$$I_\nu = 5.8 \times 10^{-18} \left(\frac{\nu}{2 \times 10^8} \right)^{-0.7} \text{ erg cm}^{-2} \text{ ster}^{-1} \text{ sec}^{-1} \text{ (c/s)}^{-1} . \tag{96}$$

Observations in the 200 Mc/s survey by Dröge and Priester (Reference 28) revealed for $\ell^{II} = 30°$, a brightness temperature $T_b = 500°K$. This corresponds to an intensity of I_ν (observed) $= 6 \times 10^{-18}$ erg $cm^{-2} ster^{-1}$ $(c/s)^{-1}$ sec^{-1}. This is to compare with the calculated theoretical value of $I_\nu = 5.8 \times 10^{-18}$ erg cm^{-2} $ster^{-1}$ $(c/s)^{-1}$ sec^{-1}. The extremely good agreement between the observed and theoretical value is, of course, accidental, since rather crude assumptions went into the theoretical derivation. Nevertheless, it proved that the synchrotron process is able to explain the observed spectral distribution of the galactic and extragalactic non-thermal radio radiation and also that the observed absolute intensities are reasonably well represented under certain assumptions for the energy distribution of the cosmic ray electrons and for a galactic magnetic field of 10^{-5} gauss.

The Lifetime of Relativistic Electrons

The energy losses of fast electrons moving through interstellar matter (H atoms and ions, $N = 0.1$ cm^{-3}) are due to the following processes:

a) magneto-bremsstrahlung (cyclotron and synchrotron emission),

b) bremsstrahlung due to Coulomb collisions between electrons and protons,

c) ionization of atoms,

d) the inverse Compton effect, i.e., scattering of fast electrons on thermal photons of the insterstellar radiation field in the galaxy.

For electrons with energies $E < 10^{10}$ ev, loss due to d) $\ll$ loss due to b). For electrons with energies $E > 10^{10}$ ev, loss due to the inverse Compton effect is comparable to the loss due to Coulomb bremsstrahlung, but still small compared to the loss due to magneto-bremsstrahlung in a magnetic field of 10^{-5} gauss, which is believed to be characteristic for the interstellar space. Because the atom densities we are concerned with are very small, and the electron energies very large we can neglect the loss due to ionization compared with the loss due to magneto-bremsstrahlung. Table 2 [from Ginzburg (Reference 17)] gives a comparison between the energy losses due to the respective processes.

a) *the lifetime of an electron,* calculated on the basis of energy loss by *synchrotron emission.* The total power emitted is given by Equation 64:

$$P = \frac{2}{3} \frac{e^2 \dot{v}^2}{c^3} \left(\frac{E}{m_0 c^2} \right)^4 \text{ erg sec}^{-1} . \tag{64}$$

Table 2

Energy Losses of Electrons in ev sec^{-1} due to the Following Processes.*

Electron Energy in ev	Ionization $N = 0.1\ cm^{-3}$	Coulomb Bremsstrahlung $N = 0.1\ cm^{-3}$	Synchrotron Radiation $H = 10^{-5}$ Gauss
10^8	2.8×10^{-8}	8×10^{-9}	4×10^{-9}
10^9	3.3×10^{-8}	8×10^{-8}	4×10^{-7}
5×10^9	3.7×10^{-8}	4×10^{-7}	10^{-5}
10^{10}	3.9×10^{-8}	8×10^{-7}	4×10^{-5}
5×10^{10}	4.3×10^{-8}	4×10^{-6}	10^{-3}

*After Ginzburg (Reference 17).

Remembering that $\dot{v} = v^2/R = v \cdot \omega = v\,(eH/m_0 c)(m_0 c^2/E)$, we find for $v = c$,

$$P = 6.2 \times 10^{-27} \times H^2 \times E^2 \text{ erg sec}^{-1} , \tag{97}$$

where E is in ev and H in gauss. So

$$\frac{dE}{dt} = -P = -3.8 \times 10^{-6} H^2 E^2 \text{ Bev sec}^{-1} , \tag{98}$$

where E is in Bev and H again in gauss. Integration of Equation 98 between $t = 0$ and $t = t$, letting the initial energy be E_0 yields:

$$\frac{1}{E(t)} = 3.8 \times 10^6 H^2 \times t + \frac{1}{E_0} . \tag{99}$$

Hence

$$E(t) = \frac{E_0}{3.8 \times 10^{-6} H^2 E_0 t + 1} \text{ erg} . \tag{100}$$

The half-life of the electron being defined by $E(t_{1/2}) = 1/2\,E_0$, we find

$$t_{1/2} = \frac{1}{3.8 \times 10^{-6} \times H^2 E_0} \text{ sec} = \frac{8.4 \times 10^{-2}}{H^2 \times E_0} \text{ years} , \tag{101}$$

where E is in Bev and H in gauss.

Table 3 gives the electron half-lives for different values of H and the initial energy E_0.

Table 3

Electron Half-Lives and Critical Frequencies for Several Electron Energies.

	Electron Energy in ev	$t_{1/2}$ in Years	ν_c in Mc/s	λ_c
$H = 10^{-5}$ Gauss	10^8	8×10^9	1.6	~200 m
	10^9	8×10^8	1600	~2 m
	10^{10}	8×10^7	1.6×10^4	~2 cm
	10^{12}	8×10^5	1.6×10^8	~2×10^4 Å
	10^{14}	8×10^3	1.6×10^{12}	~2 Å
$H = 10^{-3}$ Gauss	10^{13}	8	1.6×10^{12}	~2 Å

RADIOGALAXIES AND QUASI-STELLAR RADIO SOURCES

General Description

Although the first detection of radio waves from outer space was in 1932 by Jansky, it was not before 1946 that a *discrete* source was observed (Reference 2). The first tentative identifications with optically known objects were made by Bolton, Stanley and Slee (Reference 31) who identified the radio sources Taurus A, Centaurus A and Virgo A with the Crab nebula (NGC 1952, NGC 5128 and NGC 4486 respectively). But it was only in 1952, when Baade and Minkowski identified the radio source Cyg A with a peculiar galaxy which seemed to consist of two galaxies in collision and also studied several other objects extensively, that astronomers generally accepted the identifications (Reference 3). Up to the present time there are 1159 sources listed by Mills, Slee and Hill (Reference 32) and 328 in the revised 3rd Cambridge catalogue (Reference 33), of which so far only 70 have been identified with visible objects. We will discuss in this chapter only the extragalactic radio sources that have been identified with optically observed objects. Many radio sources will probably never be identified because their distances are too large for the associated object to be found on the photographic plates.

Normal galaxies like our own and the Andromeda Nebula (M 31) have a total power in the radio frequencies (between 10 and 10^4 Mc) between 10^{38} and 10^{40} erg sec^{-1}. Their radio luminosity is comparatively low. They are therefore difficult to observe when they are at large distances. Of about 50 identified sources only 8 were found to be normal. The term "normal" is here defined to mean that the ratio of optical to radio emission is in the same range as for the closest neighbor galaxies. It is expected that the majority of all galaxies will be weak radio sources, i.e., normal galaxies, and that only a rather small group constitutes the "radio galaxies" which are much easier to detect due to their extensive radio luminosity. The total power emitted from radio galaxies in the frequency range from 10 to 10^4 Mc extends up to 10^{45} erg sec^{-1}. They therefore constitute the majority of the *observed* radio sources.

It is now generally accepted that the main process which generates radio emission with continuous spectra in the meter wavelength range in galaxies is synchrotron emission. Matthews, Morgan and Schmidt (Reference 34) investigated how identified radio sources are distributed among the different types of galaxies. They studied 52 objects. Their results are described in more detail in Table 4.

The *weak* sources are mostly spiral and irregular galaxies like our galaxy, the Andromeda nebula, and the Magellanic Clouds. They are so far always single radio sources with a simple structure, centered in the galaxy, but often surrounded by an extensive halo.

The strong sources so far seem to be all related to certain special types of galaxies, namely to the D galaxies, DE type galaxies, dumbbell galaxies, N galaxies and to the quasi-stellar objects which have much smaller dimensions than the bright galaxies.

a) *D type galaxies* have the following characteristics: a bright nucleus, mostly not flattened, which is surrounded by an extensive envelope. The very large giant D galaxies are often the dominating objects of the clusters of galaxies. D galaxies frequently have diameters three to four times as large (40 - 80 kpc) as the other members. Their optical luminosities cover a range of a factor 10, but their radio luminosities differ within a range of 10^4. Although all have the distinctive nucleus and the extended envelope, there are large differences in size, the nuclei sometimes consist of two or more condensations, sometimes the cluster of galaxies itself is elongated in the same way as the envelope of the dominating D galaxy. Often absorbing dust bands are visible, revealing rotational symmetry. However, no optical feature indicates whether or not a giant D type galaxy should be a strong radio source or not.

Table 4

Range of Radio Luminosity for Different Types of Galaxies.*

Galaxy Type	Number	Percentage %	Radio Luminosity in erg sec^{-1}	Optical Power
Weak Sources				
Spirals, Irregulars	8	15	10^{38} - 10^{40}	average galaxy
Ellipticals	2	4	10^{40} - 10^{41}	10^{42} erg sec^{-1}
Strong Sources				
DE type	13	25	10^{40} - 10^{43}	
D type	16	30	10^{42} - 10^{45}	giant galaxy
db type	5	10	$10^{41.7}$ - 10^{43}	10^{44} erg sec^{-1}
N type	4	8	10^{43}	
Quasars	4	8	10^{44} - 10^{45}	10^{46} erg sec^{-1}

*The classification is made according to Morgan's scheme (Reference 35).

The correlation between D galaxies that are radio sources and those which belong to clusters is interesting. 50 percent of all D type radio sources belong to clusters, but only 5 percent of all D type galaxies in clusters are radio sources. This might perhaps indicate that a D type galaxy becomes a strong radio emitter only for a rather short period, possibly because of some catastrophe occurring inside its nucleus. If we assume the lifetime of a D type galaxy (or better its nucleus as it characterizes the galaxy) to be 10^9 years as a reasonable estimate, then we find that it would spend 5×10^7 years as a radio source.

The weakest of the D, DE type galaxies show a simple radio structure, the more luminous ones are identified with double or more complex sources.

The diameters of the D sources (or their components) are, just like the case of the weak sources, comparable to the optical size of the parent galaxy. Only very large halo sources and very strong double or multiple sources extend much farther; the separations of the components of the double sources are up to about ten times larger than the size of the galaxy.

b) *The DE type galaxies* indicate a transition between the elliptical and the D galaxies, i.e., these include all variations of the nucleus slowly fading into the envelope. It is remarkable that galaxies of DE type, closely resembling the D galaxies have a higher absolute radio luminosity than the ones resembling the elliptical galaxies.

c) *db type galaxies* (i.e., dumbbell galaxies) are very similar to the D type, the only difference is that there are *two* about equal very distinct nuclei contained in the same envelope. Their radio luminosity range is about equal to that of D sources. Three of the radio sources identified with db galaxies are single and only two are double radio sources. This indicates a rather large proportion of single sources compared with the general case of radio galaxies where only 5 to 10 percent are single radio sources. However the statistical sample is still rather small.

d) *The N type galaxies* have very bright and small nuclei, the radiation whereof constitutes most of the optical luminosity. They have very faint nebulous envelopes, often just visible as a streak, and never far extended. Their radio luminosity is on the average higher than the luminosity of the D sources, however this may be due to selection effects. They are closely related to the compact galaxies observed by Zwicky (References 36, 37 and 38), characterized by a very small nucleus, only to be distinguished from stars by the lack of the diffraction pattern on the photographic plate. These compact galaxies seem to exist over a wide range of optical spectral types. Here too are no visible differences between the strong radio sources among them and the normal ones. Zwicky (Reference 38) suggested that the quasi-stellar radio sources are the most luminous, extreme cases of these compact galaxies.

The N sources probably have a complex radio structure, with several small components which seem to be rather long and narrow (Reference 34). Since only a few have been found, and their angular diameters are very small, more refined instruments are necessary to resolve their structure well.

e) *Quasi-stellar radio sources ("quasars").* The main optical features of the quasi-stellar radio sources are:

1) they can only be distinguished from stars by their unusual excess brightness in the blue of the spectrum extending into the ultraviolet,

2) their spectra show emission lines with similarities to the emission lines of planetary nebula. Often the lines are very broad and have a very large redshift,

3) occasionally very faint wisps or jets can be optically distinguished on the photographic plates,

4) their radio diameters are usually very small, about 1".

We shall return to a more detailed description of the quasars later in this chapter.

Description of Individual Objects

We will now discuss several of the more closely studied radio galaxies.

Centaurus A, NGC 5128

The galaxy NGC 5128, identified with the radio source Centaurus A, is a DE type galaxy with a very extended envelope. The distance of Cen A is about 4.7 Mpc. The nucleus is elliptical with a broad absorbing band containing dust and gas in the equatorial region. This band is rotating about the major axis of the nucleus, like the nucleus itself, but with a larger velocity (Reference 39).

The weak extensions of the optical features along the axis of rotation are very peculiar; they reach out to more than 40 kpc and turn into the region of the radio emission. The only plausible explanation for the extension of matter along the rotational axis seems to be the ejection of material (ionized gas) along a magnetic field that might be aligned with the rotational axis.

The radio source shows a rather complex and very extended elongated structure. It extends over about 9 degrees on the sky. This corresponds to a diameter of 650 kpc. (The diameter of the Milky Way is about 30 kpc.) The detailed brightness distribution of Figure 11 shows at least 3 double sources in the extended

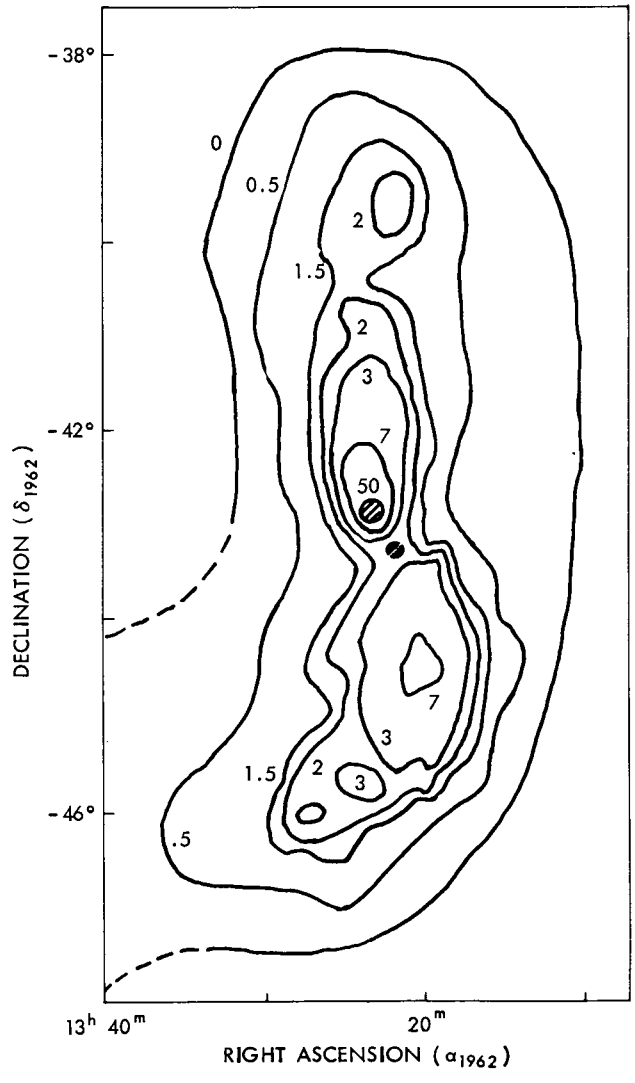

Figure 11—Centaurus A (outer sources). The brightness distribution in Centaurus A at 21.3 cm. The small black dot in the center equals approximately the galaxy as shown in Figure 12 (Reference 42).

source, and the so-called "inner source" close to the galaxy. This might indicate that these components were ejected by the galaxy during 4 successive events. This galaxy represents a special class of radio galaxies—another outstanding member of this class is Fornax A, associated with the galaxy NGC 1316. These objects generally seem to have very large linear diameters in both their optical and their radio size. Their radio luminosities are in the range of 10^{42} erg sec^{-1}. Matthews, Morgan and Schmidt (Reference 34) give the following values

$$\text{Cen A: } L = 10^{41.87} \text{ erg sec}^{-1}$$

$$\text{For A: } L = 10^{41.27} \text{ erg sec}^{-1}$$

for the range 10 to 10^5 Mc.

The polarization of the radio emission has been carefully studied, together with the depolarization effects occurring in the outer envelopes of Cen A or along the line of sight (References 40, 41 and 42). The inner source is highly polarized, in some wavelengths up to 13 percent, but the polarization is generally restricted to rather small areas. The two components are not polarized to the same degree as can be seen from Figure 12. Comparing the position angles of the axis of the nucleus, the double source closest to the nucleus and the magnetic field, we find differences, but they are confined within an angle of about 30°.

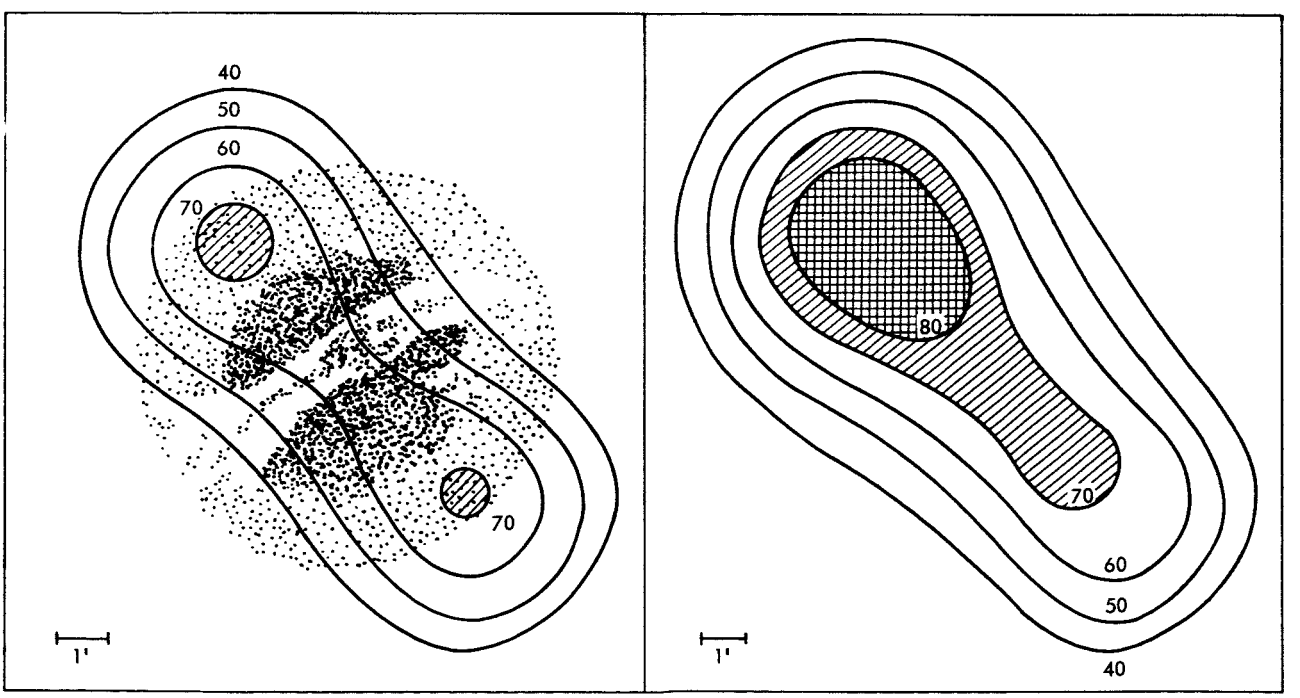

Figure 12—Centaurus A (inner source). The central part of the radio source Centaurus A at a wavelength of 10 cm. The two drawings show the measured brightness distribution for two different polarization angles. In the left part the position angle of the electric vector is 25°, in the right part 115° (adapted from Reference 40).

Fornax A, NGC 1316 (D type galaxy)

This source was identified by Mills (Reference 32). It is in many ways similar to Cen A. It also shows some absorption features across the nucleus that curve up on one side and down on the other. Arp (Reference 43) was able to obtain photographical evidence of very faint luminous extensions. Further away from the galaxy they curve towards the centers of the double radio source connected with it. The diameter of NGC 1316 as it is usually seen on photographic plates (see insert, Figure 13) is of the order of 20 kpc, in the case of Cen A (NGC 5128) it is about 25 kpc.

Polarization experiments showed that the magnetic field was not aligned with the line connecting the centers of the two radio components. It is now clear that the magnetic field follows quite well the shape of the optical extensions. The linear size of the radio emission area of Fornax A can be expected to cover up to 200 × 300 kpc. Thus it is comparable to Cen A. The main difference in the radio structure is that Cen A has several double sources and the inner source which is very close to the nucleus, while For A consists apparently only of one extended double source (Reference 44) (See Figure 13).

Perseus A, 3C84, NGC 1275

The center of a strong radio source was found to be in the Perseus galaxy cluster and identified with the peculiar galaxy NGC 1275. It appears a tightly wound spiral but it has an extended envelope and a very bright nucleus. Several condensations and outward radiating streaks are visible indicating violent events inside the nucleus of this galaxy. Its nucleus has typical "Seyfert" characteristics and shows strong emission lines exhibiting irregular features; the hydrogen Balmer lines being emitted from a region just outside the nucleus are very broad. This suggests that inside the nucleus large turbulent motions exist, and that hydrogen clouds are moving away from the center at high speeds of the order of 3000 km sec^{-1}. As the galaxy is situated in a cluster, these high velocities might be due to a collision between two galaxies; however no nucleus of a possible other galaxy colliding with NGC 1275 can be seen.

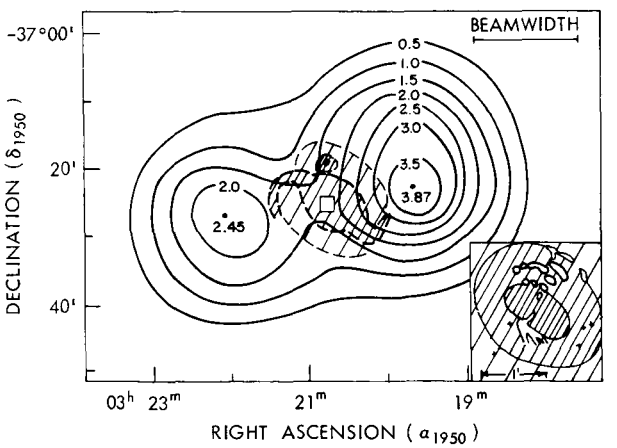

Figure 13—Fornax A (NGC 1316). The radio contours of Fornax A are from Wade (Reference 44). The large optical features are sketched from a photograph published by Arp (Reference 43). The square in the center contains the bright part of the galaxy NGC 1316. This part is given in the lower left corner ten times enlarged. There the brightness contours and the absorption patterns are sketched from the Cape Photographic Atlas of Southern Galaxies. The large optical features of NGC 1316 on the photograph envelope the SO p galaxy NGC 1317, the position of which is indicated by a dot 6.5' north of the center of NGC 1316.

The radio source Per A has a very small core, somewhat smaller than the galaxy (20 kpc) and a very extended halo of about 90 kpc or perhaps even much larger (References 45 and 46). The central source accounts for 80-85 percent of the radio luminosities, the halo provides the remaining 15 percent.

A radio galaxy quite similar to NGC 1275 is *NGC 1086*, associated with the source *3C71*. It is also a "Seyfert galaxy," its nucleus is very small and extremely bright, and the emission lines are broadened, indicating strong large scale movements in the center. The extended structure shows spiral arms, and there is some evidence of a hydrogen flare, escaping from the nucleus.

The interesting feature of NGC 1086 is that it is a comparatively weak radio galaxy of exceedingly small diameter, its radio luminosity is about 10^{40} erg sec^{-1}, placing it between the normal and the radio galaxies, the diameter of the source (600 pc or less) is much less than the diameter of the galaxy (~15 kpc).

Cygnus A is the brightest extragalactic radio source in the sky in the meter wavelength range. It was discovered by Hey (Reference 2). In 1952 Baade and Minkowski (Reference 3) identified this source with a faint object (apparent visual magnitude 15^m). The redshift in the emission lines is 0.056, corresponding to a recession speed of 16,800 km/sec. Using a Hubble constant of 100 km sec^{-1} Mpc^{-1}, we obtain a distance of about 170 Mpc. The optical diameter is about 8 kpc. The optical spectrum of Cyg A is very similar to that of the Seyfert galaxies, although the broadening of the lines is not as large as in the case of NGC 1275 and the emission comes from a region larger than the emitting regions in other Seyfert galaxies. Its optical power in the emission lines is 2×10^{44} erg sec^{-1}, its total power about 4×10^{44} erg sec^{-1} (Reference 47).

The radio source is double with two about equal components approximately 34 kpc in diameter and with a separation of 79 kpc. The components are extended along the major axis, on the center of which the galaxy is located. A polarization up to 8 percent has been measured. The direction of the magnetic field, however, is uncertain because of depolarization effects and Faraday rotation inside and outside the source (Reference 48). The radio luminosity is $10^{44.7}$ erg sec^{-1}. Cyg A is one of the brightest galaxies observed so far, in both the optical and the radio frequency range.

Virgo A, NGC 4486 (M 87)

Bolton, Stanley and Slee (Reference 31) identified Virgo A with the galaxy M87 (= NGC 4486), a member of the Virgo cluster. Baade and Minkowski (Reference 3) investigated M 87 on the Mt. Palomar 200 inch plates and especially its optical jet which protrudes from the nucleus. The galaxy is surrounded by a very large number of globular clusters. The nucleus of the galaxy is bright and small (~100 pc). The total envelope also encloses the jet and has a diameter of 6 kpc. The distance between the outermost condensation in the jet and the center is 1100 pc. As Virgo A is a strong source, polarization measurements were carried out on the jet to find out if this peculiarity is associated with the source. The jet condensations were found to be optically highly polarized, but with slightly different directions (References 49 and 50). The optical spectrum of the jet shows a blue continuum, without emission lines, similar to the Crab Nebula. This gives strong evidence that the optical radiation from the jet is also due to synchrotron radiation. There is also ionized gas present in the nucleus since there appear strong emission lines of O II that show double features, indicating that large amounts of gas are moving away from the nucleus at speeds that are, however, still comparable to the random motion inside the nucleus.

The radio source has a rather complex structure: it has been resolved in two components:

1) an unpolarized core source which is double with a separation of 2.5 kpc (Reference 51). The core source is elongated in the direction of the jet, another indication of the importance of the jet as part of the radio source,

2) a halo source emitting about 50 percent of the radio radiation. The halo is slightly polarized and has a diameter of about 20 kpc.

3C33

The peculiarity of this object is that it is a double radio source where the components have a very small size compared to their separation. It is a DE type galaxy with angular dimensions of $3''.3 \times 8''.4$. It has an outer envelope also of elliptical form ($22'' \times 9''$), but with its major axis aligned with the minor axis of the nucleus. The galaxy is probably rotating about the major axis of the envelope. The major axis of the double source forms an angle of 35° with the axis of the envelope. Polarization measurements of the radio source show that it is highly polarized, with the direction of the magnetic field in between the axes of the galaxy and the source. The separation of the components is 200 kpc (3'.8), the size of the components which are elongated along the axis is 7×14 kpc ($8'' \times 16''$) (Reference 52). The strong polarization and the small size of the components show a highly aligned magnetic field which is strong enough to confine the relativistic electrons to a rather small region.

Quasi-Stellar Radio Sources (Quasars)

In the introduction we stated already that for several years (from 1960 through 1962) the quasi-stellar radio sources were believed to be peculiar stars within our own galaxy. This was due to their perfect star-like appearance on photographic plates.

The main breakthrough in the identification came with Maarten Schmidt's paper (Reference 4) on the radio source 3C 273. The source coincides in position with a rather bright (13^m) star-like object. He was able to explain the optical spectrum when he accounted for a redshift of 0.158 corresponding to a nominal velocity of 47,400 km/sec. After this discovery, 4 more sources belonging to the same class were soon reinvestigated, as they had already been identified with stellar-like objects. These are 3C 48, 147, 196, 286.

By December 1963 the number had increased to 9 objects. The additional 4 objects are 3C 47, 245, 9 and 216. 3C 47, however, has a larger radio diameter equal to about 1 minute of arc.* The term "3C" refers to the 3rd Cambridge catalogue of radio sources (Reference 33).

The identification of the source 3C 273 was facilitated by the fact that the spectrum shows the Balmer series down to H epsilon. The appearance of 5 Balmer lines is quite unusual for these kinds of objects. A further peculiarity is that the forbidden O II line at 3727 A, which is usually very strong, is extremely weak here.

*At the second Texas Symposium on Relativistic Astrophysics (Dec. 1964) A. Sandage announced that 25 quasi-stellar objects have been found from their ultraviolet excess.

The star-like object is accompanied by a faint wisp or jet. The jet has a width of 1" - 2" and extends away from the star in position angle 43°. It is not visible within a distance of 11" from the "star" and ends abruptly at 20" from the "star."

Fortunately this radio source was occulted by the moon three times in 1962, on April 15, August 5, and October 26. The occultations were observed with the 210 ft. radio telescope at Parkes, Australia, by Hazard and associates (Reference 53) at 136, 410 and 1420 Mc/s. This led not only to the so far most accurate determination of the position, but also to a determination of the inner structure of the source. It consists of two components, designated A and B. B is associated with the star-like object, A with the jet (Figure 14). The source B seems to consist of a bright but small core with a width of 0".5, producing about 80 percent of the radio emission, and a halo of circular or elliptical shape with a width of about 7". The source A seems to have a similar structure, with a somewhat elliptical shape with the major axis in the direction towards component B. According to new eclipse observations, the difference in position between the star-like object and source B is less than 0".5.* This is so extremely small that one cannot doubt the identification, in particular since the source A coincides with the optical jet within the same accuracy.

From the lunar occultation measurements, Hazard and collaborators were able to derive the relative intensity of the two components at 410 and 1420 Mc/s and at 136 Mc/s. The ratio at the latter frequency, however, is highly uncertain. Using these data and the intensities measured by Mills at 85 Mc (Reference 32) and by Dent and Haddock at 8000 Mc (Reference 54) one can draw the radio spectrum of the entire source and the more uncertain spectra of the individual components (Figure 15). As Dent and Haddock pointed out, the spectrum of the component B resembles a thermal spectrum whereas A shows a typical spectrum of magneto-bremsstrahlung (synchrotron emission).

If one, however, follows their idea to explain the B spectrum by thermal emission, one arrives at highly unlikely results. Under the assumption of thermal emission, one can derive the temperature, electron density and total mass of the gaseous matter, if one knows the distance and the angular diameter of the source. The observed redshift, interpreted as purely cosmological, leads to a distance of about 5×10^8 pc.

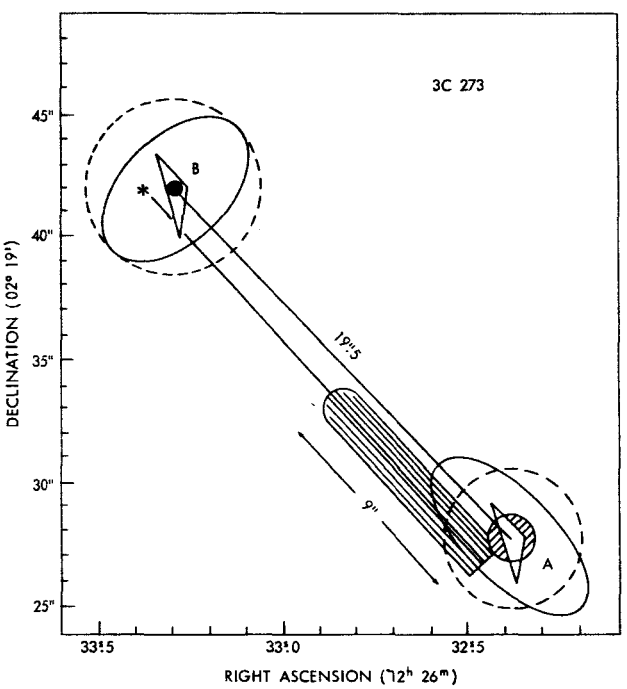

Figure 14—Optical and radio features of 3C 273. The "star" designates the position of the optically bright object; the large hatched area, the faint jet. The circles (A, B) show the positions of the related radio sources each consisting of a luminous core (inner circle) and a halo of elliptical or spherical shape. The triangle gives the edges of the moon during the 3 occultations in 1962, determining the high accuracy of the radio positions (see Reference 53).

*A. Moffett, private communication.

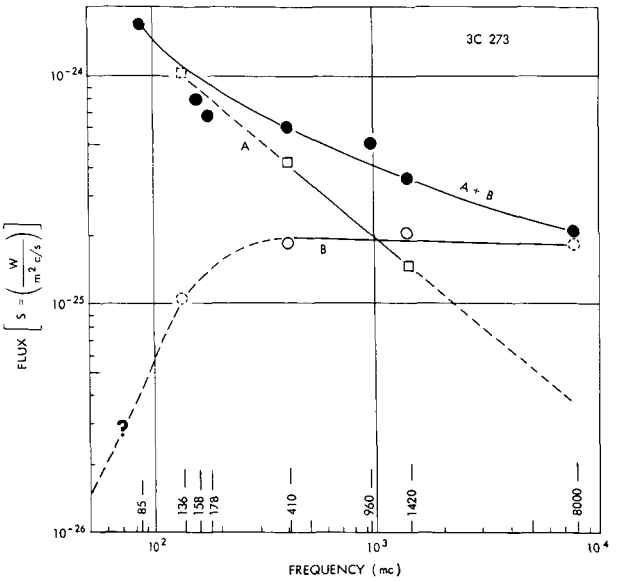

Figure 15—Radio spectrum of 3C 273. The black dots are measurements of both components. The squares give the spectrum of component A; the open circles of component B. The line through the open circles shows how one could fit a thermal spectrum to it, but this interpretation seems highly unrealistic (see text).

The diameter of the core of B which emits 80 percent of the radiation was measured to be 0.5". This corresponds to a linear diameter of 1.3 kpc. From the shape of the spectrum, one easily sees that an optical thickness equal to one is reached at about 200 Mc. Below this frequency, where the slope is 2, the radiation emerges from an optically thick layer. The flux of 6×10^{-26} W/m^2 c/s at 100 Mc/s yields a temperature of 4×10^9 °K. Furthermore $\tau = 1$ at 200 Mc/s yields an electron density of 10^5 cm^{-3} and a total mass of 10^{12} $M_\odot$.

If one assumes that the real diameter is only 1/10 of the observed upper limit, then the temperature would have to be increased to 4×10^{11}, the electron density to 10^7 cm^{-3}. The total mass would be 10^{11} $M_\odot$.

All these numbers are so large that an interpretation of the radio spectrum of component B as thermal emission seems to be very unlikely. On the other hand, an interpretation such as magneto-bremsstrahlung requires either an envelope of ionized gas with sufficiently high electron densities roughly on the order of $N_e = 10^7$ cm^{-3} which absorbs the lower frequencies (below 100 Mc) or that the energy spectrum of the relativistic electrons must have a cut-off towards the lower energies. For example, in a field of 10^{-5} gauss, the cut-off would have to occur at about 2×10^9 ev.

Immediately after Maarten Schmidt's finding of the large red shift in 3C 273, Greenstein (Reference 55) reexamined the spectrum of 3C 48. This spectrum does not show a Balmer series, but applying a redshift of 0.368 corresponding to an expansion velocity of 111,000 km/sec, he could identify the forbidden lines of O II, Ne III and Ne V. The strongest line in the spectrum then appeared at 3830 A, which belongs to ionized Mg with an unshifted wavelength of 2800 A.

Recently Maarten Schmidt found other star-like radio sources with still larger redshifts: 3C 47 with a redshift of 0.425 corresponding to a nominal velocity of 127,000 km/sec and 3C 147 with a redshift of 0.54 corresponding to 162,000 km/sec. According to Schmidt and Matthews (Reference 56) the spectrum of 3C 47 is similar to 3C 48, but the angular diameter of the radio source is much larger, about 1 minute of arc corresponding to 400 kpc. This size corresponds already to the largest double source radio galaxies. One might speculate whether the star-like radio sources are just another phase in the evolution of a radio galaxy. The redshift of 3C 147 is still somewhat tentative, since the two strong lines could also be explained with a redshift of 0.229. But this is less likely.

Figure 16 shows the schematic spectra of the 5 star-like radio sources with identified redshifted spectra (3C 273, 3C 48, 3C 47, 3C 147 and 3C 286) together with the spectra of the famous radio galaxies Cyg A and 3C 295. The peculiarity of 3C 273 is that the forbidden O II line (3727 A) is so weak that it hardly can be seen on the spectra and therefore was not listed in Schmidt's original paper. Very recently, Greenstein and Schmidt (Reference 57) published an excellent detailed analysis of the radio sources 3C 48 and 3C 273.

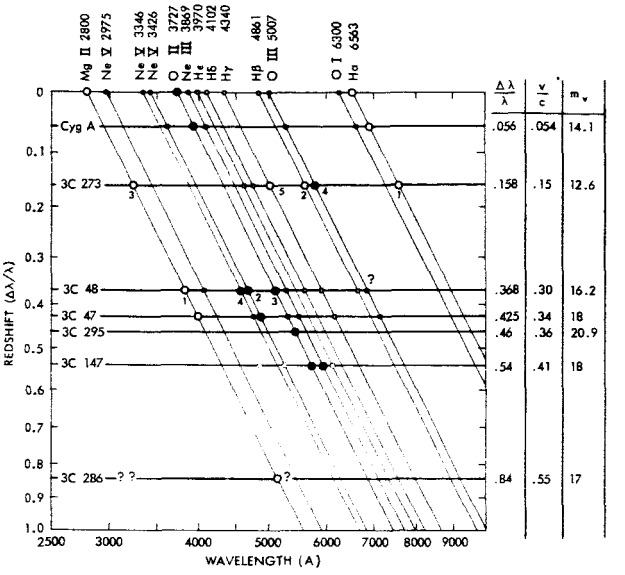

Figure 16—Schematic spectra of the quasars 3C 273, 48, 47, 147 and 286, together with Cyg A and 3C 295. The ordinate is the redshift $\Delta\lambda/\lambda$. The scale is logarithmic in $1 + \Delta\lambda/\lambda$ (adapted from Reference 55). Forbidden lines are represented by black dots. The numbers underneath the dots indicate the relative strength of the lines (number 1 being the strongest line in the spectrum). The redshift of 3C 147 is labeled as tentative, but the most likely between two possibilities (Reference 56). The redshift of 3C 286 is extremely uncertain, since there is only one line observed and no other evidence available. The identification with the Mg II 2800 Å line was proposed by Shklovsky. On the right the following data are given:

column 1: the observed redshift $\Delta\lambda/\lambda$,
column 2: the nominal "recession speed" v/c obtained by inserting $\Delta\lambda/\lambda$ into the Doppler formula,
column 3: the observed visual magnitude.

A few words should be said about the possibilities that the redshift is not purely cosmological, but rather gravitational. In that case, the quasars could be peculiar stars within the Milky Way, rather than far away extragalactic objects. But a close examination of the implications of gravitational redshift rules this possibility out. The gravitational redshift depends on the ratio of mass to radius. Greenstein derives for 3C 48 with $Z = 0.367$ a radius R (in km) $= 4\ M/M_\odot$ and a radius R(in km) $= 9\ M/M_\odot$ for 3C 273 with $Z = 0.158$

A star with about 1 solar mass and a reasonable surface brightness and a diameter of 10 km would have to be so close that its proper motion should have been observed. Jefferys of Yale University, however, reported (Reference 58) that there is no proper motion more than half the mean error of the determination. He used 14 plates from 1887 through 1963. The absolute proper motions he obtained are about 0.001 ± 0.0025 sec of arc per year. This yields a lower limit for the distance of 2×10^4 pc; therefore, the object is outside of the galaxy.

Another piece of evidence in the same direction is provided by Williams of the University of California in Berkeley. At the Symposium on Gravitational Collapse in Dallas 1963 he reported (Reference 59) about observations of the 21 cm line absorption of the galactic hydrogen situated between the source 3C 273 and the Earth. Unfortunately the source is in the constellation Virgo at the large galactic latitude of 64°. Therefore the line of sight does not intersect dense hydrogen clouds. But it seems that all hydrogen, which can be observed in emission in the surrounding of

the direction toward the source, appears in absorption, when the telescope is pointed on the source. The effect, however, is rather marginal.

A strong argument against gravitational redshift is the fact that there are strong forbidden lines which can only originate in highly dilute gases, but hardly in an atmosphere of a small object with extremely high density. A further argument is that the spectral lines are rather sharp (their widths correspond to about 50 km/s). If the lines, indeed, originate in an object with a 10 km diameter, the variation of the redshift within the layer, from which the lines are emitted, would cause much broader lines.

Therefore one can use the redshift as cosmological distance indicator with good confidence. Using these distances, one finds that these star-like objects are by far the brightest objects in the universe. Table 5 gives the nominal speed, the observed visual magnitudes and the absolute magnitudes based on a Hubble constant of 100 km sec^{-1} Mpc^{-1} and on an assumed linear relation between redshift and distance. Furthermore two values for redshift-corrected luminosities are given. The first (- 2 $\Delta\lambda/\lambda$) is the necessary minimum correction, the second (- 5 $\Delta\lambda/\lambda$) applies for a spectral energy distribution in a normal galaxy. Since the star-like objects appear to have high intensities in the blue and UV range, the necessary correction would probably lie in between the two given values. For comparison the corresponding data for the two giant radio galaxies Cyg A and 3C 295 are also given, and so are the absolute magnitudes of the brightest observed elliptical galaxy and our own galaxy. It is evident that the star-like objects are about 100 times brighter than normal giant galaxies. Typical values for the total emission in the optical and the radio range were already given in Table 4.

Table 5

Apparent and Absolute Magnitudes of 3 Quasi-stellar Radio Sources and Two Radio Galaxies.*

Object	cz 10^3 km/s	m_v	M_v	$M_v - 2\frac{\Delta\lambda}{\lambda}$	$M_v - 5\frac{\Delta\lambda}{\lambda}$
3C 273	47.5	12.6	-25.6	-25.9	-26.4
3C 48	110	16.2	-24.5	-25.2	-26.3
3C 47	127	~18	-23	-24	-25
Cyg A	16.8	14.1	-21.5	-21.6	-21.8
3C 295	138	20.9	-20.1	-21.0	-22.4
Brightest elliptical galaxy:				-22.7	
Our galaxy :				-21.0	

*Two red shift corrections on the absolute magnitudes have been given, in between which the true values can be supposed. For comparison, the absolute magnitudes of the brightest elliptical galaxy and of our own galaxy are also given.

In 1963 Matthews and Sandage (Reference 60) discovered light variations in 3C 48 and Smith and Hoffleit in 3C 273 (Reference 61). In 3C 273 there seem to exist small cyclic variations with a period of about 13 years; flashes during a week or a month during which the object is up to 1 mag brighter and in 1929 a sharp drop of 0.''4 occurred, after which the object restored to normal brightness in 1940. These variations impose a severe limit on the size in which they can occur. The 13-year cycle imposes no problem, if 3C 273 has only a diameter of about 7 light years according to the optical model by Greenstein and Schmidt (Reference 57), but the shorter variations might occur in only local regions of the object, in which case the energy content reaches very high values. Several processes have been suggested but even a supernova event would

not change the magnitude of the object appreciably, so that for the present this remains an open problem.

The sudden drop in 1929 took place in 7 months and must have occurred through the whole object, thus limiting the size of the body, where the optical radiation originates, to .3 pc, and resulting in a very high electron density in that gas cloud (Reference 57).

What can be said about the lifetimes of these radio sources? Unfortunately only crude times within several orders of magnitude can be obtained. The outer edge of the jet in 3C 273 is 1.5×10^5 light years away from the star-like object. Since it is likely that the jet originated from the star-like object, we obtain a lower limit for the lifetime of this object of 1.5×10^5 years.

Among the brightest radio sources in the 3C Catalogue, most of which (namely 25) are identified, we find 4 star-like radio sources. This corresponds to 15 percent. One might conclude from this that they either are in fact more seldom or that their lifetimes are shorter by a factor of 5 compared to the radio galaxies. This method, however, can give a hint only. The latest identifications indicate a ratio of about 2:1 between radio galaxies and quasars.

If we assume a lifetime of 10^7 years as a likely value, then the star-like objects have to provide a total energy in the form of relativistic electrons of 3×10^{58} erg. In the case of the largest radio galaxies, this value goes up even to 10^{60} erg. Since the efficiency of producing relativistic electrons cannot be very large, the actual requirements for the energy supply are still larger by at least two orders of magnitude. If one considers that 2×10^{62} erg corresponds to the rest-mass energy of 10^8 solar masses, one will be able to appreciate the difficulty in explaining the energy supply for these strange objects.

Radio Sources and Clusters of Galaxies

Recent investigations by Pilkington (1964) show that there exists a significant correlation in position between discrete radio sources and clusters. Using the new 178 Mc Cambridge survey and Abells catalogue of rich clusters, taking an area containing 435 sources, he found that 22 sources had positions within 0.4 times the radius of the cluster. Only 3 out of the 22 can be expected to be due to chance. A similar investigation using the catalogue by Mills, Slee and Hill (Reference 32), yielded 21 more coincidences, within .6 times the cluster radius, of which 5 might be due to chance. The coincidences tend to be close to the center of the cluster, which is in agreement with the fact that many D galaxies, often being close to the centers of clusters, are strong radio sources. Another point of evidence that the coincidences are real is the fact that the apparent radio flux from sources coinciding with nearby galaxies is generally larger than from those coinciding with far away clusters. There was no evidence that the richness of the cluster affects the probability of strong radio emission. A quite different picture is presented when we use only the identified radio sources (Reference 34). The results then obtained are: 50 percent of the parent galaxies occur in clusters with richness ≥ 0 and about 33 percent in clusters with richness ≥ 1, but only 20 percent appear not to be associated with clusters of galaxies; at most they might belong to very small groups. The quasars do not seem to belong to clusters, based on

the poor statistical evidence. The stronger sources tend to occur in clusters of richness 2.

This shows very clearly that one has to be very cautious in exercising statistics with these objects. On one hand many faint clusters are not included in Abell's list and therefore reduce Pilkington's coincidences (Reference 62). On the other hand, using only identified sources certainly does not present a homogeneous sample. One may conclude however that beyond any doubt there is a correlation between radio sources and clusters, the degree of correlation has yet to be determined by avoiding selection effects as much as possible.

The Radio Spectra

We will discuss here the spectra of the radio galaxies and quasars. The radio spectra of nearly all radio sources are very similar in shape and suggest strongly a great conformity regarding the processes governing the radiation of these sources in the radio frequencies. A source radiating by means of the synchrotron radiation process would have a spectrum represented by $F_\nu \sim \nu^{-\alpha_0} = \nu^{-(g_0-1)/2}$, provided that the energy spectrum of the relativistic electrons has the form $N_e(E)\,dE = A\,e^{-g_0}\,dE$ (see Equation 82). Hence plotting log F_ν versus log ν we expect to find a straight line. This is essentially confirmed by the majority of the spectra up to now obtained (References 26b, 63 and 64). The average value of the spectral index is found to be 0.74. Departures from the straight line can be explained in several ways, e.g.: 1) the electron energy spectrum is not a power spectrum, 2) the radio spectrum may be the superposition of several components.

1) Because of energy losses due to synchrotron radiation, ionization and Coulomb-bremsstrahlung, the energy spectrum of the electrons may become quite different from the spectrum of the injected electrons (the source spectrum). As these losses vary differently with energy for the different processes, the spectrum will be determined by the process responsible for the largest losses. If synchrotron radiation dominates, the spectral index will tend to $\alpha \to \alpha_0 + 1/2$; if ionization is the main process, $\alpha \to \alpha_0 - 1/2$, with all transitions possible (Reference 63). Hence in sources with very large absolute power and high temperature brightness, where we might expect relatively strong magnetic fields, the spectra will be considerably steeper than for less strong sources, where other processes may take over, which all tend to flatten the spectra.

Five of the known quasars tend to have very steep spectra, though α is never larger than 1.25, agreeing with $\alpha = \alpha_0 + 1/2$, in the extreme synchrotron radiation case. Furthermore, nearly all spectral indices lie within the $\alpha_0 + 0.5$, $\alpha_0 - 0.5$ range (i.e., between 0.24 and 1.24). This might be interpreted as a confirmation of the dependence of the spectral index on the dominating process for energy losses of the electrons (Reference 65). This outline holds only for a process of continuous supply of electrons. If the supply of relativistic electrons ends, the energy spectrum of the electrons will show a band, which will move to lower energies with increasing time. This would result in a very steep part in the radio spectrum from a certain frequency onward (dependent upon the magnetic field and time); this frequency would then also decrease with time. However no sudden steepening has been observed as yet. The currently accepted values for the intergalactic magnetic fields and the electron lifetimes would give a cut-off frequency of 10^4 - 10^5 Mc, for which no data are available as yet.

Kellerman suggests that if the electrons would be supplied from the intergalactic space, it would explain the absence of a cut-off and the remarkable similarity of the energy spectra of the relativistic electron source for many electrons in so strongly different radio sources.

2) One can easily see that for a complex source with unequal components with different spectral indices, the curvature of the integrated source will tend to be positive (compare portions A and B of Figure 14 of the radio spectrum of 3C 273) even if the curvatures of the components are negative (for low frequencies the steep component will dominate, for high frequencies the flat component). This is in good agreement with observations by Howard, Dennis, Maran and Aller (Reference 64); they found:

a) sources with positive curvature tend to be double, halo-core, or complex and of greater linear extent than sources with negative curvature. It is quite possible that all sources with positive curvature have a complex structure,

b) sources with negative curvatures tend to be smaller in linear size and in separation, and tend to have higher luminosities and surface brightnesses (Reference 66). Five quasars were found to have spectra with large negative curvature as hence could be expected. For the other quasars more data are needed.

As only few sources with positive curvature were found, and the great majority of all sources is double or complex, the components are generally expected to have a similar physical structure, and to have the same origin.

Size and Separation of Radio Sources and Their Components

The radio features of about all identified strong sources show a double or more complex structure. Maltby and Moffet (Reference 46) studied 174 extragalactic sources; they were able to resolve 75:

13 did not have a complex structure,
15 had two equal components,
40 had two or more components of unequal intensity,
7 had a bright core source and a faint halo.

Correcting for the spatial distribution, which makes us see several double-sources edge-on, we find that 80 - 85 percent of all resolved sources have double features, 10 percent are of the halo-core type, and only 5 to 10 percent are single. These percentages hold also for identified sources (Reference 34).

The double structure of nearly all strong sources is centered about the nucleus of the parent galaxy, but the components do have separations up to 360 kpc (Centaurus A). Maltby, Matthews and Moffet (Reference 67) suggested that due to some catastrophe occurring in the nucleus of the galaxy, a radio source of small diameter (1 kpc) had been ejected from the galaxy nucleus. While moving away from the galaxy the source might then expand to more than 100 kpc when having a distance of 150 kpc to the nucleus.

Many of these galaxies have a rotational symmetry, recognizable by ring-like absorbing dust bands, and sometimes actual rotation has been observed (Reference 39). Where detailed optical observations were possible faint extensions in the direction of the axis of rotation have been found. These are very peculiar features in a rotating body, and can only be explained by the presence of a magnetic field aligned with the axis of rotation, and along which a plasma has been ejected. In many cases the main axis coincides approximately with the rotational axis of the galaxy and the components are extended in the direction of that axis.

Sometimes the components are connected by an emissive bridge and show rather sharp external edges. This might be associated with the shock front of a plasma moving through a magnetic field, away from the galactic plane (Reference 68).

Since it seems obvious that the magnetic field structure of the galaxies is decisive for the structure of the sources, many experiments have recently been carried out to detect any significant polarization in the radio region. As the main emissive process in these sources is believed to be synchrotron radiation, the polarization should give some information regarding the strength and the direction of magnetic fields.

Optical polarization experiments have been carried out by Baade on Messier 87 (Reference 49) radio experiments by Westerhout (Reference 69) Bracewell and associates (Reference 40) Mayer and associates (Reference 48), Morris and associates (References 70, 71 and 72). In nearly all studied cases linear polarization of both components was found. The difference between the angles of polarization of both components was generally smaller for sources with small separations, than for sources with larger separations. This is in agreement with the model of ejected matter from the galaxy: we expect the two components to behave rather independently from each other when they have moved a considerable distance from the galaxy; close to the galaxy there will probably still be a large interaction between the two components (References 70, 71 and 72). There seems to be no simple relation between the angle of polarization and the position angle of the main axis of the double source, although there is a tendency for a 90° difference. This would then give the result predicted by the model: an alignment of the magnetic field along the axis of the source, and approximately along the axis of rotation of the galaxy.

3C 273 has two radio components, one halo-core type connected with the stellar-like object, the other component relates to the optically detected jet (see Figure 14). The source 3C 48 is single. It has a very small angular diameter (<1"). 3C 286 and 3C 196 are both probably halo-core sources, 3C 147 may be a halo-core or a double source (Reference 56). Hence, just like in the case of the optical spectra, the radio structures do not show any uniformity among the quasars. The linear sizes of the quasars and their components are generally much smaller than the other strong extragalactic radio sources, as the N galaxies and the D galaxies, which size up to 80 kpc in their optical dimensions. The diameter of the radio components ranges from < 3 kpc for 3C 48

to 10 kpc for the halo of the 3C 273 B component. The separation of the components of 3C 273 is about 40 kpc. 3C 47, the quasar with the smallest luminosity in both the optical and the radio range up to now detected, has a distance between the components of 250 kpc. This is a distance which is already in the same order of magnitude as the separations between radio components of large radio galaxies.

Cosmological Implications of Radio Source Counts

The accurate determinations of flux densities at a frequency of 178 Mc by Scott, Ryle and Hewish (Reference 73) have confirmed the earlier findings that the relationship between the number of radio sources and their flux densities is steeper than one would expect from cosmological models, which are based on the assumption of homogeneous distribution of radio galaxies in space without evolutionary effects.

Scott and Ryle (Reference 74) have shown that the number of sources plotted versus their observed flux in a double logarithmic scale can be represented by a straight line with a slope of 1.8.* This holds true for a flux range from 2 to 100×10^{-26} Watt m^{-2} $(c/s)^{-1}$ at 178 Mc. For smaller fluxes below 10^{-26} W m^{-2} $(c/s)^{-1}$ a flattening of the slope is indicated in an investigation by Hewish (Reference 75). He applied a special method proposed by Scheuer which allows the extension of the search below the limit of the observation of individual sources. The flattening of the slope was confirmed in direct observations with an instrument of greater resolution for a small area of the sky (Reference 76).

A slope of 1.8 in the number-flux relation cannot be explained with the models derived from relativistic cosmology or steady-state cosmology (References 77, 78 and 79) without introducing evolutionary effects. There is only little quantitative difference between the number-flux relations calculated for various simple cosmological models, but they all show a curved relation which starts at large flux densities with a slope of 1.5 and then bends over to smaller values.

In these investigations the distribution of radio luminosity can reasonably be represented by an effective luminosity. This takes into account that the brighter sources are sampled from a larger volume if they are counted as function of the flux density. The luminosity functions derived by Ryle show that the effective total emission in the radio frequencies ($10 - 10^4$ Mc) is in the range of 10^{43} to 10^{44} erg sec^{-1}. If there is a high percentage of quasars among the observed radio sources this value for the effective luminosity might somewhat increase.

The requirements for evolutionary effects in the radio sources have been investigated by Oort (Reference 80) (1961) and Davidson (Reference 79). In order to represent the observed slope of 1.8 one can either assume that radio sources were in the past more numerous per unit volume of the universe or that their effective luminosity was considerably larger in the early times of the evolution of the universe. Of course both possibilities can contribute in part.

*In order to have a positive slope it is assumed that the flux scale is increasing to the left side in the number-flux diagram.

From the formulas given by Priester (Reference 78) one can easily derive a lower limit for the requirements of the evolutionary effect if one requests obtaining a slope steeper than 1.5. We shall give here the relation for the Einstein-de Sitter model with euclidean metric and a cosmological constant $\Lambda = 0$. In this model the expansion is proportional to $(t_0 - T)^{2/3}$ where t_0 is the present age of the universe as defined in this model and T the time counted from the present time into the past. T is used to characterize the travel time for the radio waves from the source until they reach the observer.

The requirement for the time dependence of the number densities of radio galaxies per unit volume is

$$n = n_0 \left(\frac{t_0}{t_0 - T}\right)^a \tag{102}$$

where the exponent $a > 4$. For the luminosities the requirement is less severe

$$P = P_0 \left(\frac{t_0}{t_0 - T}\right)^b \tag{103}$$

where $b > 8/3$, n_0 and P_0 are the present values for the number density and luminosity derived from the closest objects.

If we assume an age of the universe of 10^{10} years we find that for times of 3, 5 or 7×10^9 years ago, the required number density of radio galaxies was more than 4, 16 or 120 times larger than at present. The corresponding values for the required luminosities are 2.6, 6.3 or 30 times the present luminosity for 3, 5 or 7×10^9 years ago, respectively. Because of the singularity of the model for $T = t_0$ one is, of course, not permitted to extend this result up to that time. From the numbers given it is apparent that in particular for the luminosities, the required increase in the past does not seem to be unreasonable, in particular since there is also the possibility that both the numbers and the luminosities were larger then. This, of course, would lessen the requirements on each of them correspondingly. In any case it must be kept in mind that the estimates given above can only provide some insight into the order of magnitude required for evolutionary effects.

Physical Processes

We will discuss here only the strong sources, following the discussion on this subject as presented by M. Ryle at the URSI Assembly 1963. We have to divide the processes into two classes, relating to different problems: 1) source of energy, necessary to produce these high luminosities, 2) processes to explain the spatial distribution of the radio emission or of the magnetic fields. Further the emitted power and the shape of the spectrum must be explained if one assumes the existence of a source of energetic particles and a magnetic field.

1) The main problem with the strong sources is that they require, even with modest estimates of their lifetimes, very large total energies. Theories which try to provide the energy from external sources, for instance from collisions between galaxies or even with large clouds of antimatter, are less favoured nowadays than those based on processes within the galaxy. All have to explain a total energy of the order of 10^{58} - 10^{60} ergs, supplied in the form of relativistic electrons. This value is obtained as follows: the lifetime of the relativistic electrons causing the radio frequency radiation is of the order of 10^7 years, if the magnetic field has a field strength of $H = 10^{-5}$ gauss and if the initial energy of the relativistic electrons is of the order of 10^9 ev. As these sources emit between 10^{41} and 10^{45} erg sec^{-1} in the radio range and up to 10^{46} erg sec^{-1} in the optical range, the energy supplied in the form of relativistic electrons is of the order of 10^{59} erg, if the lifetime is correctly estimated. From this one can conclude that the total energy for the largest sources is likely to exceed 10^{61} erg since there will surely be only a small percentage of the total energy stored in relativistic electrons.

Supernova explosions cannot explain this amount of high energy electrons, if they occur at the same rate as they explode in our galaxy, which is 1 every 300 years. One explosion yields about 10^{51} erg, of which only a very small portion could be converted into high energy electrons. In 10^7 years this would only yield 10^{56} erg.

A collision between two giant galaxies would not be able to supply the required energy either. Let their masses be 10^{11} solar masses, and their relative velocity 500 km/sec. Then the collision energy is 6×10^{59} erg but here too only a very small part of the energy would be transfered into high energy electrons.

Proposed mechanisms for radio galaxies and quasars involve supernovae explosions or the gravitational collapse of a superstar.

Shklovksy (Reference 9a and 9b), Burbidge (Reference 81) and Cameron (Reference 82) argue convincingly that a plausible way to obtain a sufficient number of relativistic electrons is to assume an excessively higher supernova rate during some periods within the evolution of the galaxy. Shklovksy assigns this to an early stage of the galactic evolution. Burbidge assumes that a chain reaction of Type I supernovae in the very dense central regions of a galaxy can provide the necessary frequency of explosions. In this close-packed cluster of old stars the explosions are triggered by the shock waves from the exploding neighbor stars. It seems not implausible that the required very high star densities might be found in the nuclei of D galaxies, N galaxies or perhaps in quasars.

Strong radio galaxies are usually of the D and N types, which can be considered as a special form of elliptical galaxies. This fact favors also the suggestion by Cameron (Reference 82) who assumes that intense supernova activity can arise in these galaxies during the star formation process in a large gas cloud. The more massive stars contract quickly and all spend about 3×10^6 years on the main sequence in the Hertzsprung-Russell diagram. Subsequent evolution will be rapid and will lead to Type II supernovae within a relatively short period (of the order of 10^7 years).

Hoyle and Fowler (Reference 83) try to derive the required energy from a gravitational collapse of an excessively massive superstar (10^6 to 10^8 solar masses). This suggestion is in particular of importance in connection with the quasars. The difficulties of this idea are that the contraction will lead to a rotational crisis, a faster and faster rotation which will break up the object into smaller objects. On the other hand this provides a possibility for explaining the variations in the optical emissions, as Hoyle argued at the Symposium on Gravitational Collapse in Dallas 1963. If there are large numbers of subcondensations formed, which will reach their luminous stage statistically distributed, one might expect noise-like light variations. A more detailed account on the ideas of explaining the physics of radio galaxies or quasars might be found in the reports on the Dallas symposium by Chiu (Reference 1) and Weidemann (Reference 84) or in the proceedings of the symposium edited by Robinson, Schild and Schücking (Reference 85).

ACKNOWLEDGMENTS

We are grateful to Dr. Alan T. Moffet for his suggestions for improvements.

REFERENCES

1. Chiu, H.-Y., "Gravitational Collapse," *Phys. Today*, 17(5):21-34, May 1964.

2. Hey, J. S., Parsons, S. J., and Phillips, J. W., "An Investigation of Galactic Radiation in the Radio Spectrum," *Proc. Roy. Soc.* Ser. A, 192:425-445, February 18, 1948.

3. Baade, W., and Minkowski, R., "Identification of the Radio Sources in Cassiopeia, Cygnus A, and Puppis A," *Astrophys. J.* 119:206-214, January 1954.

4. Schmidt, M., "3C 273: A Star-like Object with a Large Redshift," *Nature*, 197(4872):1040, March 16, 1963.

5. Chandrasekhar, S., "Radiative Transfer," Oxford: Clarendon Press, 1950.

6. Jackson, J. D., "Classical Electrodynamics," New York: John Wiley and Sons, Inc., 1962.

7. Kramers, H. A., "Theory of X-Ray Absorption and of the Continuous X-Ray Spectrum," *Phil. Mag.* 46:836-871, November 1923.

8. Unsöld, A., "Physik der Sternatmosphären," Berlin: Springer-Verlag, 1955.

9a. Shklovskii, I. S., "Cosmic Radio Waves," Cambridge: Harvard University Press, 1960

9b. Shklovskii, I. S., "Radio Galaxies," *Astron. Zh.* 37(6):945-960, November-December 1960 (In Russian).

10. Elwert, G., "Der Absorptionskoeffizient an der langwelligen Grenze des kontinuierlichen Röntgenspektrums," *Zeit. Naturforsch.* 3a:477-481, August-November 1948.

11. Oster, L., "Emission, Absorption, and Conductivity of the Fully Ionized Gas at Radio Frequencies," *Rev. Mod. Phys.* 33(4):525-543, October 1961.

12. Sharpless, S., and Osterbrock, D., "The Nearest H II Regions," *Astrophys. J.* 115(1):89-93, January 1952.

13. Oort, J. H, "Radio-Frequency Studies of Galactic Structure," in: *"Handbuch der Physik, Astrophysik IV: Stellar Systems,"* Vol. 53 (S. Flügge, ed.): 100-128, Berlin: Springer-Verlag, 1959.

14. Schott, G. A., "Electromagnetic Radiation," Cambridge: University Press, 1912.

15. Alfven, H., and Herlofson, N., "Cosmic Radiation and Radio Stars," *Phys. Rev.* 78:616, June 1, 1950 (Letter).

16. Kiepenheuer, K. O., "Cosmic Rays as the Source of General Galactic Radio Emission," *Phys. Rev.* 79:738-739, August 15, 1950 (Letter).

17. Ginzburg, V. L., "Cosmic Rays as a Source of Galactic Radio-Radiation," Dokl. Akad. Nauk, SSSR, 76(3):377-380, 1951 (In Russian); *Fortschr. der Phys.* 1(12):659-706, 1954 (In German).

18. Meyer, P., and Vogt, R., "Electrons in the Primary Cosmic Radiation," *Phys. Rev. Letters,* 6(4):193-196, February 15, 1961.

19. Meyer, P., and Vogt, R., "The Primary Cosmic-Ray Electron Flux during a Forbush-Type Decrease," *J. Geophys. Res.* 66(11):3950-3952, November 1961.

20. Earl, J. A., "Cloud-Chamber Observations of Primary Cosmic-Ray Electrons," *Phys. Rev. Letters,* 6(3):125-128, February 1, 1961.

21. Earl, J. A., "Cloud-Chamber Observations of Galactic and Solar Cosmic Ray Electrons," in: *"Space Research III,"* (W. Priester, ed.): 688-691, Amsterdam: North Holland Publishing Co., 1963.

22. Panofsky, W. K. H., and Phillips, M., "Classical Electricity and Magnetism," 2d ed., Reading, Mass.: Addison-Wesley Publishing Co., 1962.

23. Jäger, J., and Wallis, G., "Die Berechnung von Energiever teilungen relativistischen Elektronen aus ihrer Synchrotronstrahlung," *Beitr. Plasma Phys.* 1(1):44-63, 1960-1961.

24. Schwinger, J., "On The Classical Radiation of Accelerated Electrons," *Phys. Rev.* 75:1912-1925, June 15, 1949.

25. Wallis, G., "The Determination of the Energy Distribution of Relativistic Electrons by the Frequency Distribution of their 'Synchrotron Radiation'," in: *"Paris Symposium on Radio Astronomy, July 30-August 6, 1958; Proceedings,"* (R.N. Bracewell, ed.): 595-597, Stanford: University Press, 1959.

26a. Conway, R. G., "A Survey of the Spectra of Radio Sources," in: *Physics of Nonthermal Radio Sources,* (ed. by A.G.W. Cameron and S.P. Maran) Washington, D.C.: National Aeronautics and Space Administration SP-46, June 1964.

26b. Conway, R. G., Kellerman, K. I., and Long, R. J., "The Radiofrequency Spectra of Discrete Sources," *Month. Not. Roy. Astron. Soc.* 125( ):261-284, 1963.

27. Baldwin, J. E., "A Survey of the Integrated Radio Emission at a Wave-Length of 3.7 M," *Month. Not. Roy. Astron. Soc.* 115(6):684-689, 1955.

28. Dröge, F., and Priester, W., "Durchmusterung der Algemeinen Radiofrequenzstrahlung bei 200 Mhz," *Zeit. Astrophys.* 40(4):236-248, 1956.

29. McGee, R. X., Slee, O. B., and Stanley, G. J., "Galactic Survey at 400 Mc/s between Declinations -170° and -49°," *Austral. J. Phys.* 8(3):347-367, September 1955.

30a. Westerhout, G., "A Survey of the Continuous Radiation from the Galactic System at a Frequency of 1390 Mc/s," *Bull. Astron. Inst. Netherlands,* 14(488):215-260, December 31, 1958.

30b. Turtle, A. J., Pugh, J. F., Kenderdine, S., and Pauliny-Toth, I. I. K., "The Spectrum of the Galactic Radio Emission," *Month. Not. Roy. Astron. Soc.* 124( ):297-312, 1962.

31. Bolton, J. G., Stanley, G. J., and Slee, O. B., "Positions of Three Discrete Sources of Galactic Radio-Frequency Radiation," *Nature,* 164:101-102, July 16, 1949 (Letter).

32. Mills, B. Y., Slee, O. B., and Hill, E. R., "A Catalogue of Radio Sources between Declinations +10° and -20°," *Austral. J. Phys.* 11(3):360-387, September 1958.

33. Bennett, A. S., "The Revised 3C Catalogue of Radio Sources," *Roy. Astron. Soc. Mem.* 68(Pt. 5):163-172, 1962.

34. Matthews, T. A., Morgan, W. W., and Schmidt, M., "A Discussion of Galaxies Identified with Radio Sources," *Astrophys. J.* 140(1):35-49, July 1, 1964.

35. Morgan, W. W., "A Preliminary Classification of the Forms of Galaxies According to their Stellar Population," *Astron. Soc. Pacific, Publ.* 70(415):364-391, August 1958.

36. Zwicky, F., "Characteristic Dimensions of Cosmic Aggregates of Matter," *Astron. J.* 63(9): 504, November 1960 (Abstract).

37. Zwicky, F., "Eruptions Entendues dans Certains Noyaux de Galaxies et Certaines Galaxies Compactes," *Compt. Rend. Acad. Sci.* 257(16):2240-2241, October 14, 1963.

38. Zwicky, F., "New Types of Celestial Objects," *Sky and Telescope,* 26(2):83, August 1963.

39. Burbidge, E. M., and Burbidge, G. R., "Nature of the Peculiar Galaxy NGC 5128," *Nature,* 194:367-368, April 28, 1962.

40. Bracewell, R. N., Cooper, B. F. C., and Cousins, T. E., "Polarization of the Central Component of Centaurus A," *Nature,* 195:1289-1290, September 29, 1962.

41. Gardner, F. F., and Whiteoak, J. B., "Polarization of Radio Sources and Faraday Rotation Effects in the Galaxy," *Nature,* 197:1162-1174, March 23, 1963.

42. Cooper, B. F. C., and Price, R. M., "Faraday Rotation Effects Associated with the Radio Source Centaurus A," *Nature,* 195:1084-1085, September 15, 1962.

43. Arp, H., "A Technique for Faint Photography Applied to the Radio Source in Fornax," *Astrophys. J.* 139(4):1378-1380, May 15, 1964.

61. Smith, H. J., and Hoffleit, D., "Light Variations in the Superluminous Radio Galaxy 3C273," *Nature*, 198:650-651, May 18, 1963.

62. Pilkington, J. D. H., "Radio Sources and Rich Clusters of Galaxies," *Month. Not. Roy. Astron. Soc.* 128(2):103-111, 1964.

63. Kellermann, K. I., "The Spectra of Non-Thermal Radio Sources," in: *Observations of the Owens Valley Radio Observatory*, 3 Pasadena, Cal.: California Institute of Technology Press, 1964.

64. Howard, W. E., III, Dennis, T. R., Maran, S. P., and Aller, H. D., "Curvature in the Spectra of Non-Thermal Radio Sources," *Nature*, 202(4935):862-864, May 30, 1964

65. Tunmer, H., "The Relation of Cosmic Radio Emission to the Electronic Component of Cosmic Rays," *Month. Not. Roy. Astron. Soc.* 119(2):184-193, 1959.

66. Kellermann, K. I., Long, R. J., Allen, L. R., and Moran, M., "A Correlation between the Spectra of Non-Thermal Radio Sources and their Brightness Temperature," *Nature*, 195:692-693, August 18, 1962.

67. Maltby, P., Matthews, T. A., and Moffet, A. T., "Brightness Distribution in Discrete Radio Sources. IV. A Discussion of 24 Identified Sources," *Astrophys. J.* 137(1):153-163, January 1963.

68. Lequeux, J., "Mesures Interferometriques a Haute Résolution du Diametre et de la Structure des Principales Radio Sources a 1420 Mhz," *Ann. Astrophys.* 25(4):221-261, 1962.

69. Westerhout, G., "Search for Polarization of the Crab Nebula and Cassiopeia A at 22 cm Wavelength," *Bull. Astron. Inst. Netherlands* 12(462):309-311, May 5, 1956.

70. Morris, D., Radhakrishnan, V., and Seielstad, G. A., "Preliminary Measurements on the Distribution of Linear Polarization over Eight Radio Sources," *Astrophys. J.* 139(2):560-569, February 15, 1964.

71. Morris, D., Radhakrishnan, V., and Seielstad, G. A., "On the Measurement of Polarization Distributions over Radio Sources," *Astrophys. J.* 139(2):551-559, February 15, 1964.

72. Morris, D., Radhakrishnan, V., and Seielstad, G. A., "Linear Polarization Measurements of Radio Sources at 18-cm Wavelength," *Astrophys. J.* 139(2):758, February 15, 1964 (Note).

73. Scott, P. F., Ryle, M., and Hewish, A., "First Results of Radio Star Observations Using the Method of Aperture Synthesis," *Month. Not. Roy. Astron. Soc.* 122(2):95-111, 1961.

74. Scott, P. F., and Ryle, M., "The Number-Flux Density Relation for Radio Sources away from the Galactic Plane," *Month. Not. Roy. Astron. Soc.* 122(5):389-397, 1961.

75. Hewish, A., "Extrapolation of the Number-Flux Density Relation of Radio Stars by Scheuer's Statistical Method," *Month. Not. Roy. Astron. Soc.* 123(2):167-181, 1961.

44. Wade, C. M., "The Structure of Fornax A," *U. S. Nat'l. Radio Astron. Observ. Publ.* 1(6):99-111, August 1961.

45. Leslie, P. R. R., and Elsmore, B., "Radio Emission from the Perseus Cluster," *Observatory*, 81:14-16, February 1961.

46. Maltby, P., and Moffet, A. T., "Brightness Distribution in Discrete Radio Sources. III. The Structure of the Sources," *Astrophys. J. Suppl.* 7(67):141-163, October 1962.

47. Burbidge, G. R., Burbidge, E. M., and Sandage, A. R., "Evidence for the Occurrence of Violent Events in the Nuclei of Galaxies," *Rev. Mod. Phys.* 35(4):947-972, October 1963.

48. Mayer, C. H., McCullough, T. P., and Sloanaker, R. M., "Linear Polarization of the Centimeter Radiation of Discrete Sources," *Astrophys. J.* 139(1):248-268, January 1, 1964.

49. Baade, W., "Polarization in the Jet of Messier 87," *Astrophys. J.* 123(3):550-551, May 1956.

50. Hiltner, W. A., "Photoelectric Polarization Observations of the Jet in M87," *Astrophys. J.* 130(1):340-343, July 1959 (Letter).

51. Lequeux, J., and Heidmann, J., "Mesures Interferometriques de Radio Sources Extragalactiques à 1420 Mhz selan la Direction Est-Ouest," *Compt. Rend. Acad. Sci.* 253(5):804-806, July 31, 1961.

52. Moffet, A. T., "Component Shapes in Double Radio Sources," in: *Observations of the Owens Valley Radio Observatory*, 8, Pasadena, Cal.: California Institute of Technology Press, 1964.

53. Hazard, C., Mackey, M. B., and Shimmins, A. J., "Investigation of the Radio Source 3C273 by the Method of Lunar Occultations," *Nature*, 197(4872):1037-1039, March 16, 1963.

54. Dent, W. A., and Haddock, F. T., in: *Gravitational Collapse*, Proceedings of the 1st Texas Conference on Relativity, Dallas, December 1963, ed. by Ivor Robinson, Alfred Schild, and E. L. Schucking; Chicago: University of Chicago Press, in press, 1964.

55. Greenstein, J. L., "Quasi-Stellar Radio Sources," *Sci. Am.* 209(6):54-62, December 1963.

56. Schmidt, M., and Matthews, T. A., "Redshifts of the Quasi-Stellar Radio Sources 3C47 and 3C147," *Astrophys. J.* 139(2):781-785, February 15, 1964 (Letter).

57. Greenstein, J. L., and Schmidt, M., "The Quasi-Stellar Radio Sources 3C48 and 3C273," *Astrophys. J.* 140(1):1-34, July 1, 1964.

58. Jeffreys, W. H., III, "An Application of Rigorous Methods of Reduction to the Proper Motion of 3C273," *Astron. J.* 69(3):255-258, April 1964.

59. Williams, D., in: *Gravitational Collapse*, Proceedings of the 1st Texas Conference on Relativity, Dallas, December 1963, ed. by Ivor Robinson, Alfred Schild, and E. L. Schucking; Chicago: University of Chicago Press, in press, 1964.

60. Matthews, R. A., and Sandage, A. R., "Optical Identification of 3C48, 3C196, and 3C286 with Stellar Objects," *Astrophys. J.* 138(1):30-56, July 1, 1963.

76. Ryle, M., and Neville, A. C., "A Radio Survey of the North Polar Region with a 4.5 Minute of Arc Pencil-Beam System," *Month. Not. Roy. Astron. Soc.* 125(1):39-56, 1962.

77. McVittie, G. C., "Counts of Extragalactic Radio Sources and Uniform Model Universes," *Austral. J. Phys.* 10(3):331-350, September 1957.

78. Priester, W., Zur Statistik der Radioquellen in der relativistischen Kosmologie," *Zeit. Astrophys.* 46(3):179-202, 1958.

79. Davidson, W., "The Cosmological Implications of the Recent Counts of Radio Sources. II. An Evolutionary Model," *Month. Not. Roy. Astron. Soc.* 124(1):79-93, 1962.

80. Oort, J. H., "Some Considerations Concerning the Study of the Universe by Means of Large Radio Telescopes," in: *Large Antennas for Radio Astronomy* (Proceedings of the OECD Symposium held in Paris, France, 1961).

81. Burbidge, G. R., "Galactic Explosions as Sources of Radio Emission," *Nature,* 190:1053-1056, June 17, 1961.

82. Cameron, A. G. W., and Burbidge, G. R., "Star Formation in Elliptical Galaxies and Intense Radio Sources," *Nature,* 194:963-965, June 9, 1962.

83. Hoyle, F., and Fowler, W. A., "On the Nature of Strong Radio Sources," *Month. Not. Roy. Astron. Soc.* 125(2):169-176, 1963.

84. Weidemann, V., "Quasistellare Radioquellen—Dichtekrisen im Kosmos," *Naturwissenschaften,* 51(12):280-284, June 1964.

85. *Gravitational Collapse,* Proceedings of the 1st Texas Conference on Relativity, Dallas, December 1963, ed. by Ivor Robinson, Alfred Schild, and E. L. Schücking; Chicago: University of Chicago Press, in press, 1964.